In vitro and in vivo toxicological evaluation of acyl glucuronides

Atsushi Iwamura

March 2016

Dissertation

In vitro and in vivo toxicological evaluation of acyl glucuronides

Drug Metabolism and Toxicology

Division of Pharmaceutical Sciences

Graduate School of Medical Sciences,

Kanazawa University

School registration No. **1329012005**

Name **Atsushi Iwamura**

Primary supervisor name **Miki Nakajima**

LIST OF CONTENTS

LIST OF ABBRIVIATIONS

AG	Acyl glucuronide
AGE	Advanced glycation end product
ALT	Alanine transaminase
ARB	Angiotensin receptor blocker
BSO	L-Buthionine-(*S,R*)-sulfoximine
BUN	Blood urea nitrogen
cDNA	Complementary DNA
CRE	Creatinine
dKF	Dansylated lysine-phenylalanine
DMSO	Dimethyl sulfoxide
DNA	Deoxyribonucleic acid
EDTA	Ethylenediamine *N,N,N',N'*-tetraacetic acid
FBS	Fetal bovine serum
GAPDH	Glyceraldehyde 3-phosphate dehydrogenase
GSH	Glutathione
GSSG	Disulfide glutathione
H&E	Hematoxylin-eosin
HEK	Human embryonic kidney
HO-1	Heme oxygenase 1
hPBMCs	Human peripheral blood mononuclear cells
HPLC	High-performance liquid chromatography
ICAM-1	Intercellular adhesion molecule-1
IL	Interleukin
KPB	Potassium phosphate buffers
KO	Knockout
LC	Liquid chromatography
LTRA	Leukotriene receptor antagonist
Lys-Phe	Lysine-phenylalanine
MAPK	Mitogen-activated protein kinase
MCP-1	Monocyte chemoattractant protein 1
MDA	Malondialdehyde
MIP-2	Macrophage inflammatory protein-2
MPO	Myeloperoxidase
mRNA	Messenger RNA
MS	Mass spectrometry
MS/MS	Tandem mass spectrometry
MT	Metallothionein

NAD^+	Nicotinamide adenine dinucleotide
NAMPT	Nicotinamide phosphoribosyltransferase
NSAID	Nonsteroidal anti-inflammatory drug
PBS	Phosphate-buffered saline
RT-PCR	Reverse transcription polymerase chain reaction
S100A9	S100 calcium-binding protein A9
SD	Standard deviation
SEM	Standard error of mean
TBARS	Thiobarbituric acid reactive substances
TNFα	Tumor necrosis factor alpha
TOTP	Tri-*o*-tolyl phosphate
Tris	Tris(hydroxymethyl)aminomethane
UDP	Uridine 5'-diphosphate
UDPGA	UDP-Glucuronic acid
UGT	UDP-Glucuronosyltransferase
UPLC	Ultra-performance liquid chromatography
ZP	Zomepirac
ZP-AG	Zomepirac acyl glucuronide

CHAPTER 1

General introduction

Humans are exposed many drugs and non-drug xenobiotics such as dietary, environmental and industrial chemicals which are lipophilic compounds. The conversion of lipophilic compounds to more hydrophilic compounds serves as an elimination pathway (Rowland et al., 2013). UGTs are phase II enzymes that play important roles in the metabolism of a lot of lipophilic endogenous and exogenous compounds (Mackenzie et al., 2005). The glucuronidation is a major drug-metabolizing reaction and accounts for approximately 40-75% of xenobiotic elimination (Wells et al., 2004). UGTs catalyze the transfer of glucuronic acid from UDP-glucuronic acid (UDPGA) to carboxyl groups as well as hydroxyl and amine groups (Ritter, 2000) (Fig.1).

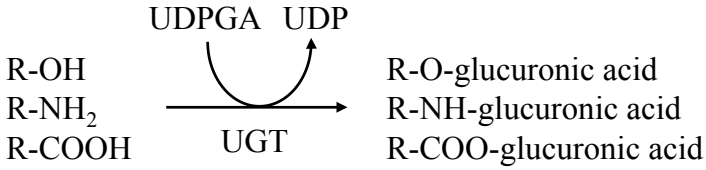

Fig. 1. Glucuronidation reaction scheme.

The formations of *O*- or *N*-glucuronides by UGTs are considered as a detoxification process because these glucuronides are generally neither active nor reactive and are excreted rapidly from the body. In contrast, acyl glucuronides (AGs) generated by glucuronidation of a carboxylic moiety are unstable and consequently undergo hydrolysis or intramolecular rearrangement through the migration of the drug moiety from the 1-*O*-position to the 2-, 3-, or 4-positions on the glucuronic acid ring (Smith et al., 1990; Benet et al., 1993; Bailey and Dickinson, 2003). It has been reported that AGs can bind covalently to proteins and other macromolecules due to their electrophilicity, suggesting that they are associated with the immunogenicity and toxicity (Spahn-Langguth and Benet, 1992). In fact, approximately 25% of drugs withdrawn from the market because of severe toxicity have been drugs containing a

carboxylic acid moiety, such as ibufenac, zomepirac and benoxaprofen (Bailey and Dickinson, 2003). To date, both direct and immune-mediated toxic pathways have been suggested as possible toxic mechanisms of AGs.

In order to assess the toxicological risks of carboxylic acid-containing drugs, the chemical stability and reactivity of AGs have been evaluated. The chemical stability was evaluated by the half-lives of AGs in potassium phosphate buffer (KPB). The half-lives of AGs in withdrawn drugs were shorter than those in safe drugs. Therefore, this assay is useful to predict the risk of toxicity (Sawamura et al., 2010; Jinno et al., 2013). Next, the reactivity of AGs was evaluated by the formation of peptide adducts. Lysine-phenylalanine (Lys-Phe), a novel trapping agent that forms glycation adducts via a Schiff base, successfully trapped the AGs of several drugs. In this assay, a correlation was observed between the formation of a peptide adduct and the rearrangement rate of the primary AG of 7 drugs (Wang et al., 2004). In addition to chemical instability, mycophenolic acid AG induced tumor necrosis factor alpha (TNFα) and interleukin-6 (IL-6) mRNA expression, and diclofenac AG induced interleukin-8 (IL-8) and monocyte chemoattractant protein 1 (MCP-1) mRNA expression in human peripheral blood mononuclear cells (hPBMCs) (Wieland et al., 2000; Miyashita et al., 2014), suggesting that the stimulation of immune cells might be involved in adverse reactions of carboxylic acid-containing drugs. It remains to be investigated whether AG-peptide adducts formation and immunostimulation are related to drug toxicities, although the predictability of the half-lives assay for drug toxicity has been evaluated (Sawamura et al., 2010; Jinno et al., 2013). In **Chapter 2**, the relationship of the results of half-lives, peptide adducts, and immunostimulation assays to the toxic category of carboxylic acid-containing drugs was evaluated, and then the usability of the three assays was compared to assess the risk of toxicity of AGs in preclinical drug discovery.

Until now, the chemical stability, the formation of covalent adducts and the immune activation have been investigated *in vitro*. However, the toxicity of AGs has remained controversial, because the direct involvement of AGs in toxicity *in vivo* has not been proved. Zomepirac (ZP), a nonsteroidal anti-inflammatory drug, was withdrawn from the market

because of their adverse effects such as anaphylaxis and nephrotoxicity (Smith, 1982; Miller et al., 1983). ZP is mainly metabolized to acyl glucuronide (ZP-AG) in human (Grindel et al., 1980; O'Neill et al., 1982). ZP-AG is more physically unstable in phosphate buffer than the other AGs of safe drugs such as gemfibrozil, repaglunide and telmisartan (Sawamura et al., 2010). ZP-AG also covalently modifies dipeptidyl peptidase IV in rat liver homogenates and microtubular protein in bovine brain in vitro as well as small peptides such as glutathione (GSH) in vivo (Bailey et al., 1998; Wang et al., 2001; Grillo and Hua, 2003). These studies suggest that ZP-AG is the cause of the toxicity induced by ZP, but it has not been demonstrated whether ZP-AG actually shows toxic effects *in vivo*. In **Chapter 3**, the relationship between the exposures of ZP and ZP-AG and the severity of ZP-induced toxicity in mice was investigated, and then the mechanism of the toxicity was analyzed.

CHAPTER 2

In vitro toxicological evaluation of acyl glucuronides utilizing half-lives, peptide adducts, and immunostimulation assays

SUMMARY

Chemical reactivity of AGs is believed to be involved in the toxicity of carboxylic acid-containing drugs. Both direct and immune-mediated toxicity have been suggested as possible mechanisms of toxicity; however, it remains unclear. In the present study, the assays of half-lives, peptide adducts, and immunostimulation were performed to evaluate the potential risk of AGs of 21 drugs and analyzed the relationship to the toxic category. AGs of all withdrawn drugs tested in this study showed short half-lives and peptide adducts formation, but so did those of several safe drugs. In contrast, only AGs of withdrawn and warning drugs induced IL-8 in hPBMCs. Using a DNA microarray assay, it was found that zomepirac AG induced the mRNAs of 5 genes, including IL-8 in hPBMCs. In addition, withdrawn and warning drugs were distinguished from safe drugs by an integrated score of relative mRNA expression levels of 5 genes. The immunostimulation assay showed higher sensitivity, specificity, and accuracy compared with other methods. In preclinical drug development, the evaluation of the reactivity of AGs using half-lives and peptide adducts assays followed by the evaluation of immunostimulation by highly reactive AGs using hPBMCs can contribute to improved drug safety.

INTRODUCTION

Acyl glucuronidation is one of the major metabolic routes of carboxylic acid-containing drugs. Glucuronidation is an important phase II metabolic pathway for endogenous and exogenous substrates and is generally considered as a detoxification pathway. However, AGs are unstable under physiological conditions and consequently undergo hydrolysis or intramolecular rearrangement through the migration of the drug moiety from the 1-*O*-position to the 2-, 3-, or 4-positions on the glucuronic acid ring (Smith et al., 1990; Benet et al., 1993; Bailey and Dickinson, 2003). Because of their electrophilic nature and capacity to cause substitution reactions with nucleophilic groups in proteins or other macromolecules, AGs can covalently modify endogenous proteins leading to the adverse toxicity associated with carboxylic acid-containing drugs (Faed, 1984; Boelsterli, 2002). Till date, both direct and immune- and inflammation-mediated toxic pathways have been suggested as possible toxic mechanisms of AGs. Previous studies (Nakayama et al., 2009; Usui et al., 2009) have reported that zomepirac and bromfenac, which are carboxylic acid-containing drugs that have been withdrawn from the market, showed low covalent binding to proteins in human hepatocytes. In addition, the AGs of the widely used drugs naproxen, diclofenac, ketoprofen, and ibuprofen did not lead to cytotoxicity or genotoxicity in UGT-transfected human embryonic kidney 293 (HEK/UGT) cells and human hepatocytes (Koga et al., 2011). In contrast, it has been reported that mycophenolic acid AG induced TNFα and IL-6, and diclofenac AG induced IL-8 and MCP-1 in leukocytes (Wieland et al., 2000; Miyashita et al., 2014), suggesting that the induction of immune modulators could lead to immune- and/or inflammation-related adverse drug reactions.

Several in vitro assay methods to assess the toxicity of AGs have been proposed. The first is an evaluation of the half-lives of AGs in KPB. The half-lives of AGs in withdrawn drugs were shorter than those in safe drugs. Therefore, this assay is useful to predict the risk of toxicity (Sawamura et al., 2010; Jinno et al., 2013). The second method is a Lys-Phe adducts assay, wherein Lys-Phe is used as a novel trapping agent that forms glycation adducts via a

Schiff base. In this assay, a correlation was observed between the formation of a peptide adduct and the rearrangement rate of the primary AG of 7 drugs (Wang et al., 2004). The third method is an immunostimulation assay using hPBMCs, wherein cytokines and chemokines, such as IL-6 and IL-8, were induced in hPBMCs by treatment with AGs (Wieland et al., 2000; Miyashita et al., 2014). Although the predictability of the assay of half-lives for drug toxicity has been evaluated (Sawamura et al., 2010; Jinno et al., 2013), the relationship between the results of the other two assays and drug toxicity remains to be investigated. The purpose of the present study was to evaluate the relationship of the results of assays of half-lives, peptide adducts, and immunostimulation to the toxic category of carboxylic acid-containing drugs defined by description in drug package inserts, and then to compare the usability of the three assays to assess the risk of toxicity of AGs in preclinical drug discovery. The assay of peptide adducts was modified by using dansylated Lys-Phe (dKF), peptide-AG adducts of which were easily detectable by fluorescence.

EXPERIMENTAL PROCEDURES

Chemicals and reagents

Oxaprozin, pranoprofen, etodolac, and dKF were prepared in-house by chemosynthesis. Probenecid was obtained from Wako Pure Chemical Industries (Osaka, Japan). Diclofenac sodium salt, tolmetin sodium salt dihydrate, zomepirac sodium salt, mefenamic acid, bumetanide, furosemide, flufenamic acid, meclofenamic acid sodium salt, ibuprofen, and repaglinide were obtained from Sigma-Aldrich (St. Louis, MO). Montelukast sodium and telmisartan were obtained from Kemprotec (Middlesborough, UK). Gemfibrozil was obtained from LKT Laboratories (St. Paul, MN). Naproxen sodium was obtained from Tocris Bioscience (Ellisville, MO). Ibufenac, benoxaprofen, piretanide, and AGs of zomepirac, benoxaprofen, tolmetin, ibufenac, diclofenac, mefenamic acid, probenecid, naproxen, gemfibrozil, furosemide, repaglinide, telmisartan, and ibuprofen were purchased from Toronto

Research Chemicals (Ontario, Canada). Pooled human liver microsomes were obtained from XenoTech, LLC (Lenexa, KS). The UGT reaction mix solution (250 mM Tris-HCl (pH 7.4), 40 mM $MgCl_2$, and 0.125 mg/ml alamethicin) was purchased from Corning Gentest (Woburn, MA). Characterized hPBMCs (lot no. LP80), uncharacterized hPBMCs (10 individuals), and CTL-Test medium were obtained from Cellular Technology (Shaker Heights, OH). TRIzol and the High-Capacity cDNA Reverse Transcription Kit were obtained from Life Technologies (Carlsbad, CA). TaqMan Universal Master Mix, TaqMan Gene Expression Assays, and Human GAPDH Endogenous Control (FAM/MGB probe, non-primer limited) were obtained from Applied Biosystems (Darmstadt, Germany). The Human IL-8 ELISA Ready-SET-GO! Kit (2nd Generation) was obtained from eBioscience (San Diego, CA). Other chemicals were analytical grade or the highest grade commercially available.

Formation of AGs and degradation in KPB in assay of half-lives

A chemical stability study was performed according to the methods described by Chen et al. (2007), with slight modifications. The test compounds were incubated at concentrations of 500 μM at 37°C for 60 min with pooled human liver microsomes (2.0 mg protein/mL) in 100 mM Tris-HCl buffer (pH 7.4) containing 10 mM $MgCl_2$, 50 μg/mL alamethicin, and 4 mM UDPGA. The volume of each reaction mixture was 300 μL, and the reaction was stopped by adding an equal volume of acetonitrile. The reaction-stopped mixture was transferred to new reaction tubes and mixed with 4 volumes of 100 mM KPB (pH 7.4). The samples were incubated at 37°C and aliquots were removed at 0, 10, 20, 40, 90, 180, and 300 min. The reaction was stopped by adding an equal volume of acetonitrile/methanol (90/10) containing 1% formic acid and the internal standard (0.2 μM niflumic acid). The reaction mixture was centrifuged at 3000 rpm at 4°C for 5 min, and then the supernatants were collected and stored at −20°C until analysis.

Liquid chromatography–tandem mass spectrometry (LC-MS/MS) analysis of AGs in assay of half-lives

To determine half-lives, the 1-*O*-β-AGs in samples prepared as described above were measured by LC-MS/MS. An Acquity system (Waters, Milford, MA) equipped with a Waters Acquity UPLC BEH C18 column (1.7 μm, 2.1 mm × 100 mm) and a triple quadrupole mass spectrometer (Quattro Premier and Xevo TQ MS; Waters) were used. The AGs were separated from other isomers and metabolites using an elution gradient. The mobile phases were 0.1% formic acid and acetonitrile. The column was eluted at a flow rate of 0.4 mL/min at 50°C. The elution program and the MS/MS condition for detection of AGs are shown in Table 1 and Table 2, respectively.

Calculating the half-lives of AGs

The degradation rate constant (*K*) of each AG was determined from the LC-MS/MS peak area of 1-*O*-β-AG versus time curve by the linear regression of the semi-logarithmic plot. The half-lives (*T1/2*) were calculated from *K* by the following equation:

$$T1/2 = \ln 2/K$$

Table 1. The elution program of LC method for separating acyl glucuronides.

Compounds	min	solvent A %	solvent B %	gradient	Compounds	min	solvent A %	solvent B %	gradient
Ibuprofen	0.0	98	2	none	Diclofenac	0.0	98	2	none
Gemfibrozil	0.5	98	2	none	Etodolac	0.5	98	2	none
	6.0	30	70	linear		1.5	60	40	linear
	6.1	98	2	none		4.5	60	40	none
	8.0	98	2	none		5.5	5	95	linear
						6.0	5	95	none
						6.1	98	2	none
						8.0	98	2	none
Compounds	min	solvent A %	solvent B %	gradient	Compounds	min	solvent A %	solvent B %	gradient
Oxaprozin	0.0	98	2	none	Repaglinide	0.0	98	2	none
	0.5	98	2	none	Bumetanide	0.5	98	2	none
	1.5	63	37	linear		1.5	65	35	linear
	4.5	63	37	none		4.5	65	35	none
	5.5	5	95	linear		5.5	5	95	linear
	6.0	5	95	none		6.0	5	95	none
	6.1	98	2	none		6.1	98	2	none
	8.0	98	2	none		8.0	98	2	none
Compounds	min	solvent A %	solvent B %	gradient	Compounds	min	solvent A %	solvent B %	gradient
Ketoprofen	0.0	98	2	none	Piretanide	0.0	98	2	none
Ibufenac	0.5	98	2	none		0.5	98	2	none
	1.5	70	30	linear		1.5	70	30	linear
	4.5	70	30	none		4.5	70	30	none
	5.5	20	80	linear		5.5	5	95	linear
	6.0	20	80	none		6.0	5	95	none
	6.1	98	2	none		6.1	98	2	none
	8.0	98	2	none		8.0	98	2	none
Compounds	min	solvent A %	solvent B %	gradient	Compounds	min	solvent A %	solvent B %	gradient
Pranoprofen	0.0	98	2	none	Others	0.0	98	2	none
	0.5	98	2	none		0.5	98	2	none
	1.5	75	25	linear		5.0	2	98	linear
	4.5	75	25	none		6.0	2	98	none
	5.5	5	95	linear		6.1	98	2	none
	6.0	5	95	none		8.0	98	2	none
	6.1	98	2	none					
	8.0	98	2	none					

Solvent A: 0.1% formic acid, solvent B: acetonitrile.

Table 2. The MS/MS condition for acyl glucuronides detection.

Compounds		Ion Mode	Q1	Q3	Compounds		Ion Mode	Q1	Q3
Niflumic acid	I.S.	ES+	283.1	245.1					
Flufenamic acid	UC	ES+	282.1	167.0	Naproxen	UC	ES+	231.1	185.1
	AG	ES+	282.1	167.0		AG	ES+	231.1	185.1
Gemfibrozil	UC	ES-	249.1	120.9	Montelukast	UC	ES+	586.2	422.2
	AG	ES-	425.0	249.0		AG	ES+	586.2	422.2
Meclofenamic acid	UC	ES+	296.1	243.1	Probenecid	UC	ES+	286.1	121.1
	AG	ES+	472.0	296.0		AG	ES+	462.1	286.1
Repaglinide	UC	ES+	453.3	230.2	Diclofenac	UC	ES+	296.1	214.2
	AG	ES+	629.3	453.3		AG	ES+	296.1	214.2
Telmisartan	UC	ES+	515.2	276.3	Mefenamic acid	UC	ES+	242.1	180.1
	AG	ES+	691.2	515.2		AG	ES+	418.0	242.0
Furosemide	UC	ES+	331.0	81.0	Tolmetin	UC	ES+	258.1	119.1
	AG	ES+	331.0	81.0		AG	ES+	258.1	119.1
Ibuprofen	UC	ES-	205.0	161.0	Benoxaprofen	UC	ES+	302.1	256.1
	AG	ES-	381.0	205.0		AG	ES+	302.1	256.1
Ibufenac	UC	ES+	193.1	147.1	Pranoprofen	UC	ES+	256.1	210.2
	AG	ES+	193.1	147.1		AG	ES+	256.1	210.2
Zomepirac	UC	ES+	292.1	110.9	Etodolac	UC	ES+	288.2	171.9
	AG	ES+	292.1	110.9		AG	ES+	464.2	288.2
Bumetanide	UC	ES+	365.2	240.2	Oxaprozin	UC	ES+	294.1	102.8
	AG	ES+	541.2	365.2		AG	ES+	294.1	102.8
Piretanide	UC	ES+	363.2	282.2					
	AG	ES+	539.2	282.2					

UC, unchanged; AG, acyl glucuronide
Q1 of acyl glucuronide is Q1 of unchanged drug or Q1 of unchanged drug + 176 Da (glucuronic acid moiety).
Q3 of acyl glucuronide is Q1 of unchanged drug or Q3 of unchanged drug.

Formation of AG-dKF adducts

The test compounds were incubated at concentrations of 500 μM with pooled human liver microsomes (2.0 mg protein/mL) in 88 mM KPB (pH 7.4) containing 8 mM $MgCl_2$, 25 μg/mL alamethicin, and 4 mM UDPGA at 37°C for 60 min. The volume of the mixture was 500 μL, and the reaction was stopped by adding 1 mL of ice-cold acetonitrile, followed by centrifugation at 14,000 rpm at 4°C for 5 min. The supernatant (1.4 mL) was transferred into another test tube, evaporated to dryness under a N_2 stream at 40°C, and resuspended in 500 μL of acetonitrile/KPB (15/85) containing 10 mM dKF. After 3 h incubation at 37°C, the mixture was evaporated to dryness under a N_2 stream at 40°C, resuspended in 500 μL of acetonitrile/water (50/50), and filtrated (0.2-μm filter) by centrifugation at 4,500 g at 4°C for 10 min. The AG-dKF adducts were analyzed by LC-mass spectrometry (MS) and fluorescence as follows.

LC-MS analysis of AG-dKF adducts

Samples prepared as described above were subjected to LC-MS. An Acquity system (Waters) equipped with a Waters Acquity UPLC HSS T_3 column (1.8 μm, 2.1 mm × 50 mm) was used. Mobile phases were 0.1% formic acid (solvent A) and 90% acetonitrile containing 0.1% formic acid (solvent B). The column was eluted at a flow rate of 0.6 mL/min at 40°C. Conditions for elution were as follows: 20% solvent B (0–1 min), 20%–50% B (1–7 min), 50%–90% B (7–13 min), 90% B (13–14 min), and 20% B (14.1–15.5 min). The dKF adducts were detected by fluorescence (excitation 340 nm, emission 525 nm) using a fluorescence detector (2475 Multi λ Fluorescence Detector; Waters) and mass spectrometry using a hybrid triple quadrupole/linear ion trap mass spectrometer (4000 QTRAP; AB Sciex, Framingham, MA). Parameters for mass spectrometers were as follows: ion mode, positive-electrospray ionization (enhanced MS scan mode); collisionally activated dissociation, high; curtain gas, 30 psi; ion source gas 1, 40 psi; ion source gas 2, 80 psi; ion source voltage, 5000 V; source temperature, 500°C; full scan mass range, 200–900 (doubly charged ion). The dKF adducts were formed via acylation or glycation. Acylation adducts and glycation adducts were detected at *m/z* M/2 + 297 and M/2 + 385, respectively, ($[M + 2H]^{2+}$; M: the molecular weight of unchanged drug). The schematics of chemical mechanisms of acylation and glycation and chemical structures of peptide adducts are shown in Figure 2.

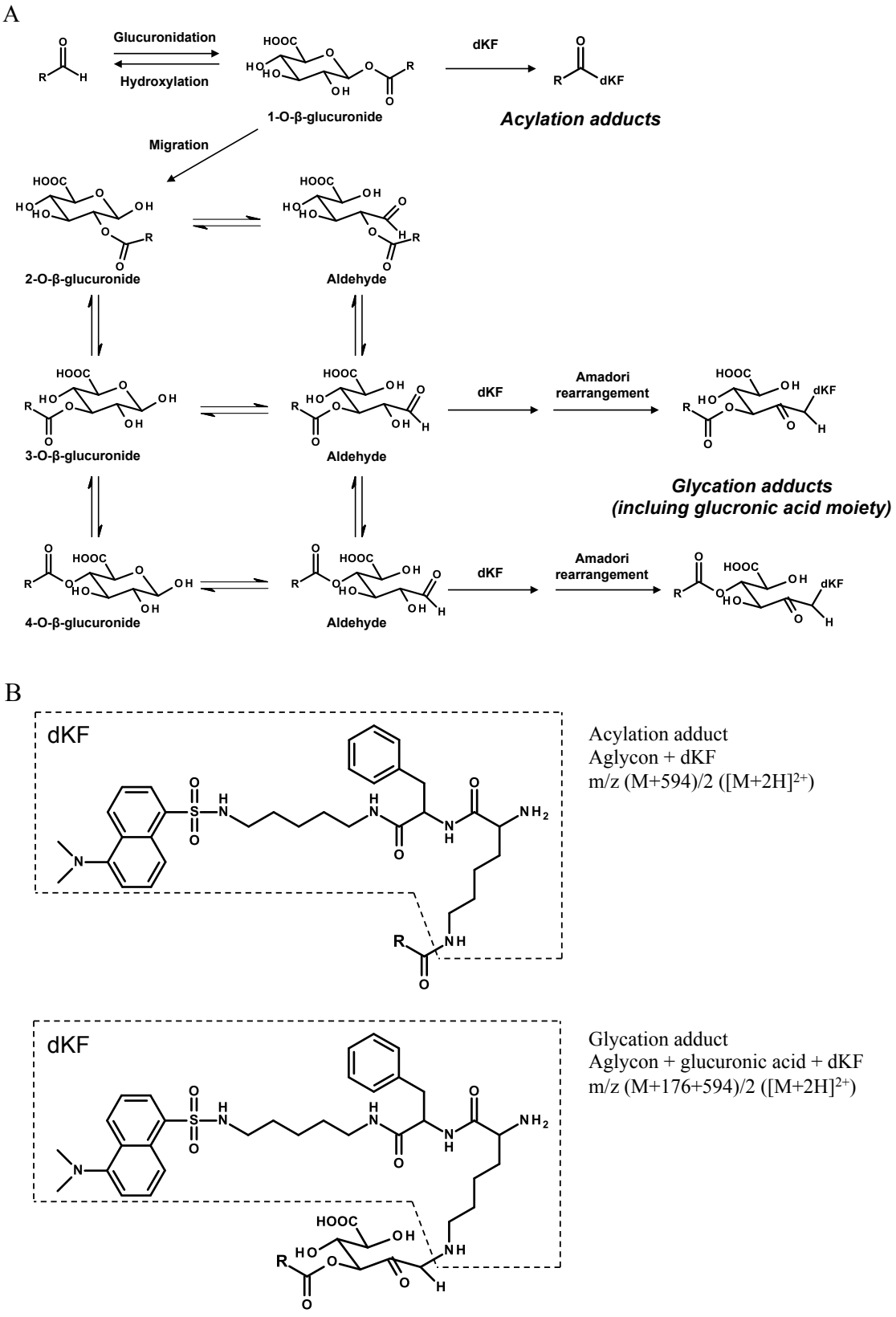

Fig. 2. The schematics of chemical mechanisms of acylation and glycation (A) and chemical structures of peptide adducts (B).

Cell culture in immunostimulation assay

The hPBMCs were maintained at 37°C under an atmosphere of 5% CO_2. For the assay, the hPBMCs were seeded at densities of 3×10^5 cells/well in a 24-well plate with medium containing 100 μM AG and then incubated at 37°C for 24 h. The AGs were dissolved in dimethyl sulfoxide (DMSO) containing 1% formic acid at 50 mM concentration, and the final concentration of DMSO in the culture medium was 0.2% in all of the experiments.

Real-time reverse transcription polymerase chain reaction (RT-PCR)

Total RNA was extracted from the cultured cells using TRIzol (Life Technologies) according to the manufacturer's protocol. The reverse transcription was performed with the High-Capacity cDNA Reverse Transcription Kit (Life Technologies) according to the manufacturer's protocol. Two microliters of cDNA was used for quantitative real-time RT-PCR, which was performed in the 7900HT Fast Real-Time PCR System (Applied Biosystems) capable of fluorescence using TaqMan Universal Master Mix (Applied Biosystems). Gene-specific oligonucleotide primers and probes for human cluster of differentiation 69 (CD69; assay ID: Hs00934033_m1), chemokine (C-X3-C motif) receptor 1 (CXCR1; assay ID: Hs01922583_s1), interferon gamma (IFNγ; assayID: Hs00989291_m1), IL-1α (assay ID: Hs00174092_m1), IL-6 (assay ID: Hs00985639_m1), IL-8 (assay ID: Hs00174103_m1), lymphocyte cytosolic protein 2 (LCP2; assay ID: Hs01092638_m1), microsomal glutathione *S*-transferase 1 (MGST1; assay ID: Hs00220393_m1), metallothionein (MT) 2A (assay ID: Hs02379661_g1), and nicotinamide phosphoribosyltransferase (NAMPT; assay ID: Hs00237184_m1) were obtained as TaqMan Gene Expression Assays (Applied Biosystems). The reaction mixture contained 10 μL TaqMan Universal Master Mix and 1 μL of the specific primer in a final volume of 20 μL. The PCR conditions were as follows: after an initial polymerase activation at 95°C for 20 seconds, the amplification was performed through 40 cycles of either denaturation at 95°C for 1 second or annealing and extension at 60°C for 20 seconds. To normalize the RNA loading and PCR variations, the signals of the targets were normalized to those of human GAPDH mRNA.

Enzyme-linked immunosorbent assay (ELISA)

The levels of the inflammatory chemokine IL-8 in cultured medium were measured using the Human IL-8 ELISA Ready-SET-GO! Kit (eBioscience), according to the manufacturer's instructions.

DNA microarray analysis

Total RNA was extracted from hPBMCs treated with 100 μM zomepirac AG, tolmetin AG (positive control), or ibuprofen AG (negative control) for 24 h using TRIzol. The total RNA concentration was calculated with an OD260 using a NanoDrop (ND-1000), and the OD260/280 was confirmed to be 1.8 or more. The integrity of total RNA was examined with a 2100 BioAnalyzer (Agilent Technologies), and its RNA Integrity Number (RIN) value was confirmed to be 6 or more. The cDNA synthesis, biotin labeling, purification, fragmentation, hybridization, and scanning of GeneChip arrays were performed according to the GeneChip 3′ IVT Express Kit user manual (Affymetrix). The biotinylated and fragmented complementary RNA was hybridized on the GeneChip Human Genome U133 Plus 2.0 Array (38,500 genes). After the hybridization, washing and fluorescence staining were performed using a Fluidics station 450 (Affymetrix). Next, the arrays were scanned using the GeneChip Scanner 3000, and the scanned images were analyzed using the Expression Console Ver.1.1 (Affymetrix). Data analysis was performed using the GeneSpring GX 12.0 software package (Agilent Technologies).

Statistical analysis

The statistical analysis of multiple groups was performed using one-way ANOVA with Dunnett's post hoc test to determine the significance of differences between individual groups. Comparisons between two groups were carried out using two-tailed Student's *t* tests. A value of $P < 0.05$ was considered statistically significant.

RESULTS

Half-lives of AGs in KPB

In the present study, the 21 carboxylic acid-containing drugs shown in Table 3 were categorized into three groups on the basis of severe adverse drug reactions as follows. The 4 drugs categorized as “withdrawn” included drugs withdrawn from the market because of their toxicity, with potential to cause hepatotoxicity and anaphylaxis. The 3 drugs with a warning about fulminant hepatitis in drug package inserts in Japan or the United States or in the summary of product characteristics in Europe were categorized as “warning.” The other 14 drugs with no warnings in drug package inserts were categorized as “safe” drugs. First, the half-lives of the 21 AGs were evaluated. The half-lives of AGs of the all withdrawn drugs were shorter than 2 h, and the AG of diclofenac, which was categorized as a warning drug, also had a short half-life. However, the half-lives of AGs of the other 2 warning drugs were longer than 2 h, and the half-lives of AGs of several drugs categorized as safe, including probenecid, bumetanide, piretanide, oxaprozin, ibuprofen, and pranoprofen, were shorter than 2 h (Table 4). Therefore, in terms of toxicity, this assay produced some false-positive and some false-negative results.

Table 3. Drugs used in the present study.

Category	Drugs	Class	Dose mg/man/day
Withdrawn	Zomepirac	NSAID	600
	Benoxaprofen	NSAID	600
	Tolmetin	NSAID	1800
	Ibufenac	NSAID	4000
Warning	Diclofenac	NSAID	200
	Mefenamic acid	NSAID	1500
	Montelukast	LTRA	10
Safe	Probenecid	Uricosuric agent	1000
	Naproxen	NSAID	600
	Gemfibrozil	Lipid regulator	1200
	Furosemide	Loop diuretic	80
	Repaglinide	Hypoglycemic agent	16
	Telmisartan	ARB	80
	Ibuprofen	NSAID	3200
	Bumetanide	Loop diuretic	2
	Piretanide	Loop diuretic	12
	Oxaprozin	NSAID	600
	Pranoprofen	NSAID	225
	Flufenamic acid	NSAID	750
	Meclofenamic acid	NSAID	400
	Etodolac	NSAID	400

NSAID: Non-steroidal anti-inflammatory drug

LTRA: Leukotriene receptor antagonist

ARB: Angiotensin receptor blocker

Table 4. Half-lives of AGs in KPB and formation of dKF adducts with AGs in human liver microsomes.

Category	Drugs	Half-lives h	dKF acylation adduct	dKF glycation adduct
Withdrawn	Zomepirac	0.5	-	+
	Benoxaprofen	1.2	-	+
	Tolmetin	0.4	-	+
	Ibufenac	1.0	-	+
Warning	Diclofenac	0.7	+	++
	Mefenamic acid	>15.0	-	-
	Montelukast	9.3	-	-
Safe	Probenecid	0.4	-	+
	Naproxen	3.1	+	-
	Gemfibrozil	>15.0	-	-
	Furosemide	3.8	-	+
	Repaglinide	11.5	+	-
	Telmisartan	>15.0	-	-
	Ibuprofen	1.8	+	-
	Bumetanide	0.3	+	++
	Piretanide	1.0	+	++
	Oxaprozin	1.1	+	
	Pranoprofen	1.9	-	-
	Flufenamic acid	7.5	++	++
	Meclofenamic acid	>15.0	+	+
	Etodolac	>15.0	-	-

++: Detected adducts more than 100 pmol/h/mg

+: Detected adducts less than 100 pmol/h/mg

-: Not detected.

Formation of dKF adducts of AGs

The production of dKF adducts was assessed by fluorescence and LC-MS. When diclofenac was incubated with dKF as a positive control, an acylation adduct and multiple glycation adducts were detected by fluorescence and MS (Fig. 3). The multiple glycation adducts of dicolofenac detected in this assay would be isomers of AGs formed via intramolecular rearrangement. Such dKF adducts were not detected in the absence of diclofenac or UDPGA. As shown in Table 4, AGs of all withdrawn drugs formed glycation adducts but not acylation adducts. For some of the safe drugs with short half-lives, acylation and/or glycation adducts were detected, although the drugs that formed neither acylation nor

glycation adducts had long half-lives, except for pranoprofen. On the whole, the formation of glycation adducts was better correlated with toxicological category than the formation of acylation adducts (Table 4). These results suggest that glycated proteins rather than acylated proteins are involved in the toxicity of AGs. However, similar to the assay of half-lives, the dKF assay could not accurately predict the toxicity of AGs.

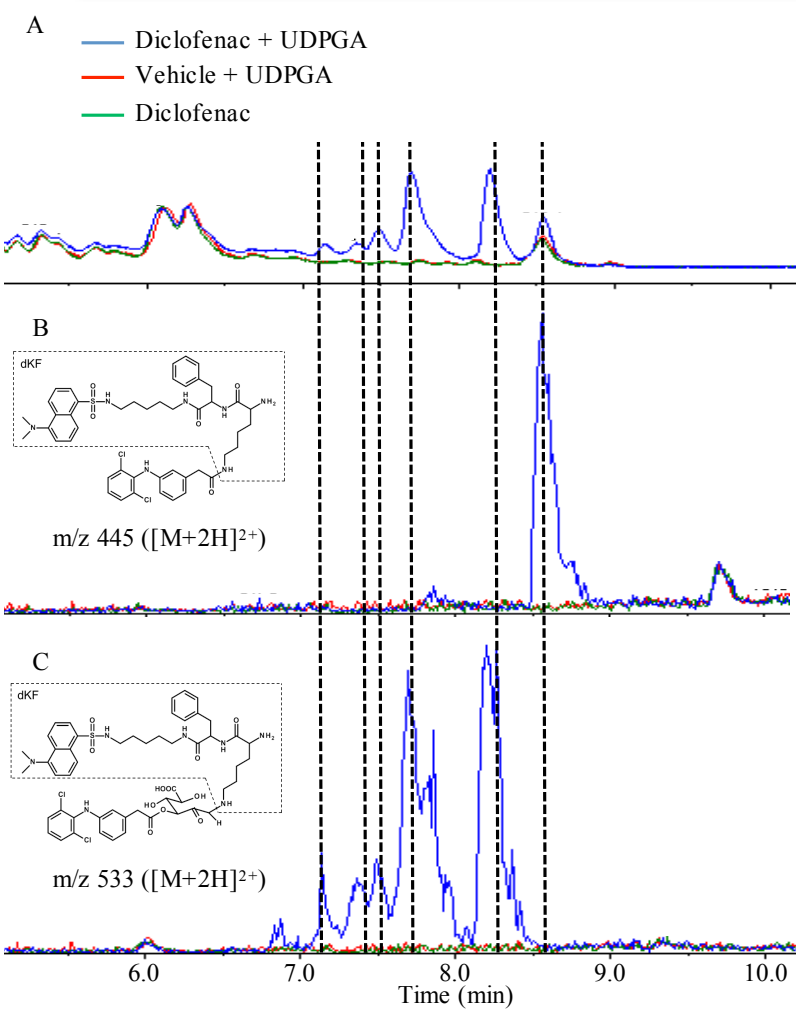

Fig. 3. Fluorescence (A) and ion chromatograms (B, C) from LC-MS analysis of the dKF adducts of diclofenac AG. (B) Extracted ion current (XIC) chromatograms of the acylation adducts of diclofenac AG at m/z 445 ($[M + 2H]^{2+}$). (C) XIC chromatograms of the glycation adducts of diclofenac AG at m/z 533 ($[M + 2H]^{2+}$). LC-MS conditions were as described in Experimental Procedures.

IL-8 mRNA induction in hPBMCs by AGs

A previous study demonstrated that exposure of hPBMCs to diclofenac AG resulted in an increase in the expression of IL-8 mRNA, suggesting that AGs could induce immune and inflammation responses (Miyashita et al., 2014). To examine whether the increase in IL-8 in hPBMCs is associated with the toxic category, the induction of IL-8 mRNA expression after treatment with AGs was evaluated for 4 withdrawn drugs, 2 warning drugs, and 7 safe drugs. The expression of IL-8 mRNA was significantly increased by AGs of all withdrawn drugs and the warning drugs mefenamic acid and diclofenac but not by AGs of any of the safe drugs (Fig. 4A). Moreover, IL-8 protein release was significantly increased by the treatment with AGs of several withdrawn drugs (Fig. 4B). These results suggest that immune and inflammatory responses are involved in the toxicity of AGs, and the induction of IL-8 mRNA in hPBMCs is a useful biomarker to evaluate the toxicity of AGs.

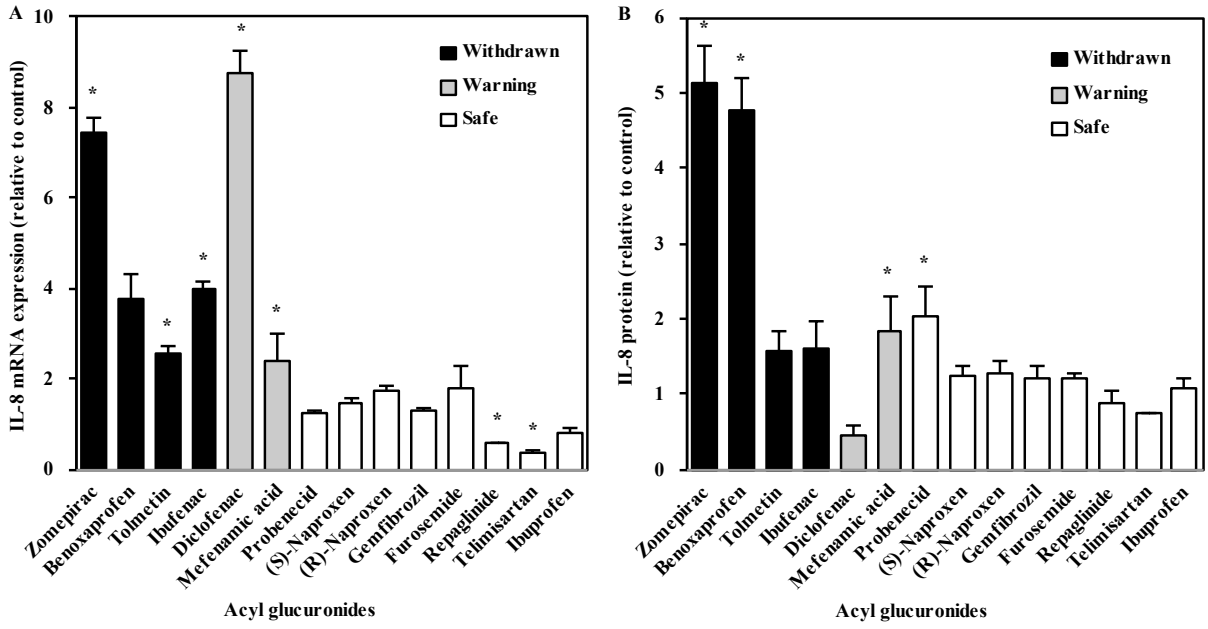

Fig. 4. Effects of AGs on the mRNA expression levels (A) and the protein release (B) of IL-8 in hPBMCs. hPBMCs were treated with 14 AGs (100 μM), or vehicle (0.2% DMSO) for 24 h. The IL-8 mRNA levels in hPBMCs and released protein in cultured medium were measured by real-time RT-PCR and ELISA, respectively, and the IL-8 mRNA levels were normalized with GAPDH mRNA as described in Experimental Procedures. The data represent relative changes to vehicle control and are the means ± SD (n = 3). *$P < 0.01$ as compared with vehicle control (Dunnett's test).

Interindividual differences among hPBMCs for IL-8 mRNA induction by AGs

For the construction of screening protocols, it is important to examine interindividual differences in responses among hPBMCs. IL-8 mRNA induction by zomepirac AG in hPBMCs from 11 different individuals was measured (Fig. 5). The upregulation of IL-8 mRNA by zomepirac AG was observed in hPBMCs from all 11 individuals; however, there was no upregulation by ibuprofen AG. There was an approximately 3.5-fold interindividual variability in IL-8 mRNA induction. Therefore, the immunostimulation by zomepirac AG could be detected regardless of the donor.

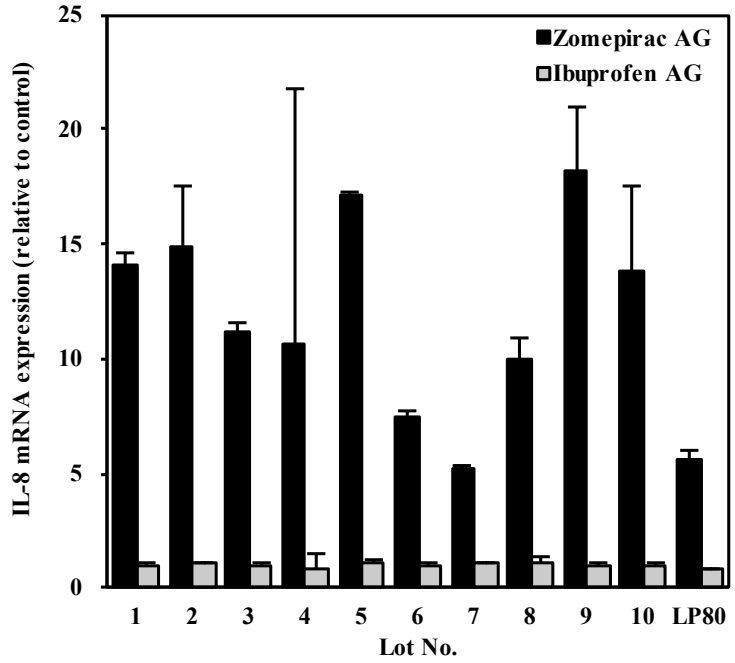

Fig. 5. Effects of zomepirac AG and ibuprofen AG on the mRNA expression levels of IL-8 in hPBMCs from 11 individuals. hPBMCs were treated with zomepirac AG, ibuprofen AG (100 μM), or vehicle (0.2% DMSO) for 24 h. The expression level of IL-8 mRNA was measured by real-time RT-PCR and normalized with that of GAPDH mRNA as described in Experimental Procedures. The data represent the means ± SD (n = 3).

Toxicological assessment by changes in multiple gene expression

A DNA microarray analysis was performed to search for biomarkers other than IL-8 for toxicity of AGs. RNA samples from hPBMCs treated with AGs of zomepirac, tolmetin, or ibuprofen were analyzed. There were 201 genes upregulated more than 1.5-fold by AGs of both zomepirac and tolmetin that were not or were less upregulated by ibuprofen AG. Among them, CD69, CXCR1, IFNγ, IL-1α, IL-6, LCP2, MGST1, MT2A (with the largest change

among the MT isoforms), and NAMPT, all of which are related to immune response or toxicity, were selected in addition to IL-8 (Table 5). The real-time RT-PCR analysis of mRNA of the 10 selected genes showed significant induction (more than 2-fold compared to vehicle control) of IL-8, IL-1α, IL-6, MT2A, and NAMPT mRNA by zomepirac AG (Fig. 6). Further evaluation was carried out using a total sum score, which was defined as an integrated score of the relative expression levels of mRNA of these 5 genes in hPBMCs treated with AGs of other drugs (4 withdrawn drugs, 2 warning drugs, and 7 safe drugs). The total sum scores of gene expression for AGs of all withdrawn and warning drugs were higher than 10, which represents a greater than 2-fold induction compared with vehicle treatment. In contrast, the total sum scores for AGs of all safe drugs were lower than 10. Therefore, this method could distinguish withdrawn and warning drugs from safe drugs when a total sum score of 10 was used as a cut-off value for safe drugs (Fig. 7).

Table 5. Summary of immune-associated or toxicity-associated genes that showed changed expression after exposure to AGs of zomepirac, tolmetin, or ibuprofen.

Gene symbol	Gene title	Fold changes		
		AGs		
		Zomepirac	Tolmetin	Ibuprofen
CD69	CD69 molecule	2.31	1.52	1.23
CX3CR1	chemokine (C-X3-C motif) receptor 1	1.98	1.62	1.26
IFNG	interferon, gamma	1.59	1.57	1.22
IL-1A	interleukin 1, alpha	17.39	3.33	2.54
IL-6	interleukin 6 (interferon, beta 2)	4.34	1.63	1.43
IL-8	interleukin 8	4.53	1.91	1.25
LCP2	lymphocyte cytosolic protein 2	2.15	1.52	1.24
MGST1	microsomal glutathione S-transferase 1	1.82	1.74	0.94
MT1E	metallothionein 1E	4.15	2.34	1.24
MT1F	metallothionein 1F	3.29	2.06	1.11
MT1G	metallothionein 1G	2.95	1.67	1.14
MT1H	metallothionein 1H	3.81	2.15	1.09
MT1X	metallothionein 1X	4.07	2.93	1.36
MT2A	metallothionein 2A	4.94	3.12	1.45
NAMPT	nicotinamide phosphoribosyltransferase	3.66	1.88	1.09

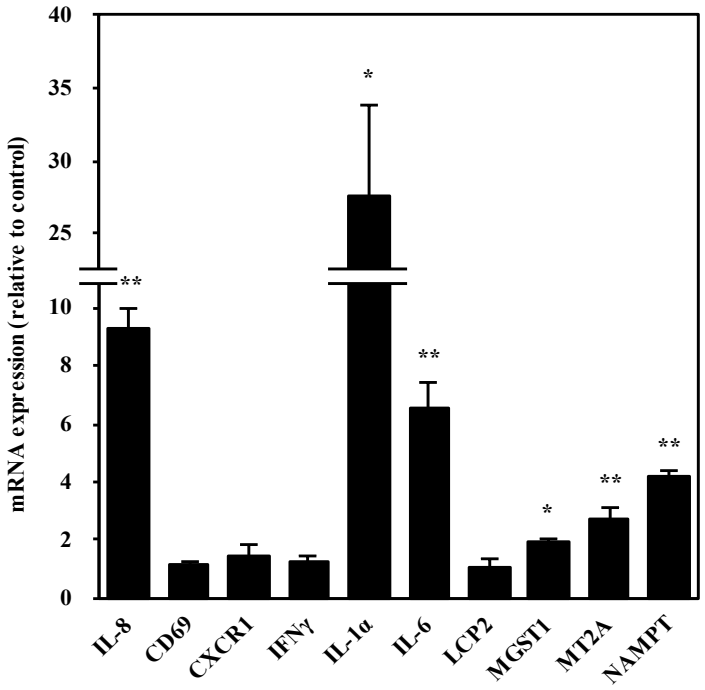

Fig. 6. Effects of zomepirac AG on the mRNA expression levels of IL-8, CD69, CXCR1, INFγ, IL-1α, IL-6, LCP2, MGST1, MT2A, and NAMPT in hPBMCs. hPBMCs were treated with zomepirac AG (100 μM), or vehicle (0.2% DMSO) for 24 h. The expression level of each mRNA was measured by real-time RT-PCR and normalized with that of GAPDH mRNA as described in Experimental Procedures. The data represent the means ± SD (n = 3). **P* < 0.05 and ***P* < 0.01 as compared with vehicle control in each gene (Student's *t*-test).

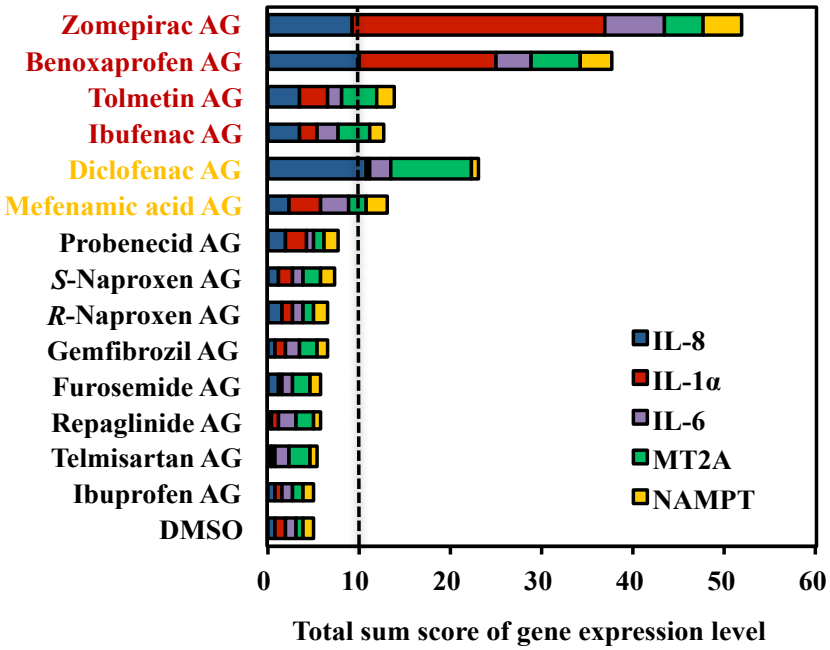

Fig. 7. Total sum score of gene expression level of 14 drugs. The total sum score of gene expression level was defined as an integrated score of the relative expression levels of IL-8, IL-1α, IL-6, MT2A, and NAMPT mRNA in hPBMCs. The expression level of each mRNA was measured by real-time RT-PCR and normalized with that of GAPDH mRNA as described in Experimental Procedures. Red indicates withdrawn drugs, orange indicates warning drugs, and black indicates safe drugs. The data represent the means (n = 3).

Comparison of half-lives, dKF adduct formation, and immunostimulation assay for toxicological assessment of AGs

The 4 withdrawn drugs were identified as toxic by all 3 assays (Table 6). However, among the safe drugs, probenecid, bumetanide, and piretanide were identified as toxic by the assays of half-lives and dKF adduct formation. Oxaprozin, ibuprofen, and pranoprofen were identified as toxic by the assay of half-lives, and furosemide, flufenamic acid, and meclofenamic acid were identified as toxic in the dKF adduct formation assay. In contrast, AGs of all 7 safe drugs examined using the immunostimulation assay were identified as nontoxic. To assess the feasibility of these assays, specificity, sensitivity, and accuracy were calculated. For the assays of half-lives and dKF adduct formation, the specificity (57%) was less than the sensitivity (71%), i.e., false-positives were more frequent than false-negatives. Interestingly, there were no false-positives or false-negatives in the immunostimulation assay. Therefore, in the present study, the immunostimulation assay was the most accurate for toxicological assessment (Table 7).

Table 6. Comparison of half-lives, formation of dKF adducts, and immunostimulation assays for toxicological assessment of AGs.

Category	Drugs	Half-lives	dKF glycation adduct	Total sum score
Withdrawn	Zomepirac	+	+	+
	Benoxaprofen	+	+	+
	Tolmetin	+	+	+
	Ibufenac	+	+	+
Warning	Diclofenac	+	++	+
	Mefenamic acid	-	-	+
	Montelukast	-	-	NA
Safe	Probenecid	+	+	-
	Naproxen	-	-	-
	Gemfibrozil	-	-	-
	Furosemide	-	+	-
	Repaglinide	-	-	-
	Telmisartan	-	-	-
	Ibuprofen	+	-	-
	Bumetanide	+	++	NT
	Piretanide	+	++	NT
	Oxaprozin	+		NT
	Pranoprofen	+	-	NT
	Flufenamic acid	-	++	NT
	Meclofenamic acid	-	+	NT
	Etodolac	-	-	NT

++: Detected glycation adducts more than 100 pmol/h/mg

+: Half-life < 2h or detected glycation adducts less than 100 pmol/h/mg or total sum score > 10.

-: Half-life ≧ 2h or not detected glycation adducts or total sum score ≦ 10.

NT: Not tested because authentic AGs were not commercially available.

NA: Not available by a decrease of GAPDH mRNA expression.

Table 7. Sensitivity, specificity, and accuracy of assays of half-lives, formation of dKF adducts, and immunostimulation.

	+	-	Sensitivity (%)	Specificity (%)	Accuracy (%)
Half-lives assay					
Withdrawn and warning	5	2	71	57	62
Safe	6	8			
dKF adducts formation assay					
Withdrawn and warning	5	2	71	57	62
Safe	6	8			
Immunostimulation assay					
Withdrawn and warning	6	0	100	100	100
Safe	0	7			

DISCUSSION

The AGs of drugs are generally unstable and are believed to be involved in drug-induced toxicity via the formation of covalent adducts to endogenous proteins. In the process of drug discovery, it is important to predict and avoid the toxicity of AGs of new chemical entities, to reduce the need to withdraw drugs from the market, and to increase safety in clinical trials. Although there is increasing evidence that AGs form drug–protein adducts via their chemical reactivity (Grubb et al., 1993; Wang et al., 2001; Horng and Benet, 2013), cytotoxicity and genotoxicity of AGs have not been observed in the in vitro assays, suggesting that the toxicity of AGs could be mediated by immune-related and/or inflammation-related responses (Koga et al., 2011). However, the toxicity of AGs has remained controversial. Therefore, in the present study, the aspects of the chemical instability, reactivity, and immunostimulation potential of AGs in a range of drugs were evaluated using assays of half-lives, dKF adduct formation, and immunostimulation, respectively.

The evaluation of half-life in KPB has been used to assess the chemical instability of AGs (Chen et al., 2007; Sawamura et al., 2010; Jinno et al., 2013). Similar to the results of previous studies, in the present study, the half-lives of withdrawn drugs tended to be short (less than 2 h). However, of particular note is the finding that AGs of some drugs categorized as safe (bumetanide, piretanide, oxaprozin, ibuprofen, and pranoprofen) also had short half-lives, indicating chemical instability. Therefore, this method may produce false-positive results. Half-lives in KPB reflect not only the degradation of 1-*O*-β-AG via hydrolysis but also the intramolecular rearrangement. It has been reported that the percentage of AG rearrangement of ibuprofen is less than that of zomepirac and tolmetin (Wang et al., 2004). Therefore, the unstable AGs of safe drugs, such as ibuprofen, may be mainly degraded via hydrolysis to aglycones and less so via intramolecular rearrangement and would have low reactivity. In contrast, it was suggested that the unstable AGs of withdrawn or warning drugs, such as zomepirac or diclofenac, were less hydrolyzed but highly formed intramolecular rearrangement resulting in formation of glycation adducts.

Next, the formation of peptide adducts using dKF was examined to evaluate the chemical reactivity of AGs with proteins. dKF is a novel trapping agent rendered detectable by fluorescence by dansylation of KF, which forms adducts with AG. Glycation adducts were detected in all withdrawn drugs tested in the present study, whereas acylation adducts were not. Consequently, the formation of glycation adducts rather than acylation adducts was suggested to correlate with toxicity. Unlike acylation adducts, glycated proteins are formed through Schiff bases and Amadori rearrangement and generate advanced glycation end products (AGEs). AGEs contribute to various diseases, including the complications of diabetes, arterial sclerosis, and liver disease, mediated by immune mechanisms (Ramasamy et al., 2005; Takeuchi et al., 2014). AGEs originating from glycated proteins may be partially involved in the toxicity of AGs. Glycation adducts were detected not only in withdrawn drugs but also in several safe drugs (bumetanide, piretanide, furosemide, flufenamic acid, and meclofenamic acid). Therefore, as for the half-lives assay, the evaluation of peptide adducts has the potential to produce false-positive results and does not accurately predict the toxicity of AGs.

In our previous study, it was found that immune- and inflammation-related genes, such as IL-8 and MCP-1, in hPBMCs were up-regulated by diclofenac AG (Miyashita et al., 2014). To investigate the immunotoxicity of AGs and to establish a novel method with high prediction accuracy, we performed an immunostimulation assay using hPBMCs. Consistent with our previous study (Miyashita et al., 2014), IL-8 mRNA induction in hPBMCs by diclofenac AG was confirmed, and significant induction of IL-8 by AGs of all withdrawn drugs was identified. Notably, the AGs of safe drugs did not induce IL-8 mRNA, showing accurate correlation with the toxic category. It was demonstrated that the parent compounds zomepirac and tolmetin did not increase the expression of IL-8 mRNA (data not shown). IL-8 is a chemokine that exhibits multiple effects on neutrophils, including induction of lysosomal enzyme release, increase in the expression of adhesion molecules, and rapid infiltration (Leonard et al., 1991; Baggiolini et al., 1994). In the previous report, dicofenac AG suggested to be involved in liver injury because there was good correlation between the concentration of

liver diclofenac AG and plasma alanine transaminase (ALT) levels in transporter KO mice (Lagas et al., 2010). Moreover, in mice in vivo study, the mRNA expression of macrophage inflammatory protein (MIP)-2 that is mouse orthologue of human IL-8 is dramatically induced in correlation with the extent of liver injury after diclofenac administration (Yano et al., 2014). Taken together, it is suggested that the toxicity caused by diclofenac AG is mediated via IL-8 induction. Furthermore, in assessment of allergen potency, IL-8 release from THP-1 cells have a high correlation with the local lymph node assay, animal model of evaluating skin sensitization, could be a useful marker (Mitjans et al., 2010). Therefore, IL-8 is suggested to be a potentially good marker for assessing the toxicity caused by AG. Moreover, the induction of IL-8 mRNA by zomepirac AG was also observed in hPBMCs from 11 different individuals, and interindividual differences were not marked (less than 4-fold). The upregulation of IL-8 mRNA by zomepirac AG was observed in hPBMCs from all 11 individuals, and interindividual differences appeared to be not marked. Thus, only the induction of IL-8 could not explain the idiosyncrasy. Idiosyncratic toxicity is thought to be caused by not a single factor but rather the complex of multiple factors. The factors include not only the compound potential but also the recipient's potential (e.g. age, sex, food, surrounding environment, genetic polymorphism etc.). The induction of IL-8 is one of the risk factors leading to idiosyncratic toxicity, and IL-1α, IL-6, MT2A, and NAMPT are newly found to potentially be the risk factors in our study. It is important to totally assess multiple factors, and selecting low potential compounds such as ibuprofen in drug discovery might result in reducing the risk of idiosyncratic drug toxicity.

To find novel biomarkers other than IL-8 to improve risk prediction, a DNA microarray assay was conducted using cDNA samples from hPBMCs exposed to AGs of zomepirac, tolmetin, or ibuprofen. Among the genes that were upregulated only by the treatment with AGs of withdrawn drugs (zomepirac and tolmetin), 10 immune- or toxicity-associated genes were selected. The mRNA of IL-8, IL-1α, IL-6, MT2A, and NAMPT was highly induced when the genes were individually analyzed by real-time RT-PCR. Based on a previous report (Yano et al., 2014) that assessed the risk of hepatotoxic and nonhepatotoxic drugs using an integrated

score of relative expression levels of several immune-associated genes, the 5 genes described above were applied as biomarkers to predict the toxicity of AGs. An integrated score of relative expression levels of selected genes enabled the discrimination of withdrawn drugs from safe drugs based on a cut-off score of 10, which represents a greater than 2-fold induction relative to vehicle controls. Furthermore, this evaluation method predicted toxicity with higher sensitivity, specificity, and accuracy than the other two methods.

IL-1α is a proinflammatory cytokine, constitutively expressed in gastrointestinal tract, lung, liver, kidney, endothelial cells, and astrocytes. It is a key mediator of autoimmune and inflammatory diseases (Garlanda et al., 2013). IL-6 is a prototypical cytokine produced by many different types of lymphoid and nonlymphoid cells, such as T cells, B cells, monocytes, fibroblasts, keratinocytes, and endothelial cells. It not only induces the differentiation of B cells and T cells but also stimulates hepatocytes to produce acute-phase proteins (Hirano and Kishimoto, 1989; Tanaka and Kishimoto, 2014). NAMPT is the rate-limiting enzyme in nicotinamide adenine dinucleotide (NAD+) biosynthesis and is implicated in the maturation of B cell precursors. This gene is up-regulated in neutrophil activation and stimulated monocytes (Skokowa et al., 2009). The induction of IL-8, IL-1α, IL-6, and NAMPT suggested that AGs of withdrawn drugs led to immune response activation, such as cytokines release, differentiation of immune cells, neutrophil infiltration, and inflammation. MTs plays important roles in scavenging reactive oxygen species and in heavy metal detoxification (Sato and Kondoh, 2002), and MT2A is one of the major isoforms of MT in humans (Haynes et al., 2013). MTs are induced not only by heavy metals but also by reactive oxygen species and cytokines such as IL-6 (Itoh et al., 1996). Therefore, in addition to immune-associated genes, MTs were also induced by AGs of withdrawn drugs.

The mechanisms underlying the effects of AGs on the immune system remain unclear. Recently, it was shown that the p38 mitogen-activated protein kinase (MAPK) pathway was involved in the increase in the expression levels of IL-8 mRNA in hPBMCs induced by AGs (Miyashita et al., 2014). In the DNA microarray analysis, other immune related factors were upregulated in addition to IL-8. Along with IL-8, the production of IL-6 in hPBMCs induced

by the stimulation of ribotoxin was mediated through p38 MAPK activation (Islam et al., 2006). Moreover, IL-1α is involved in the induction of IL-8 by osmotic stress in hPBMCs via the phosphorylation of p38 MAPK (Shapiro and Dinarello, 1995). The expression of both MT and NAMPT were increased by IL-6 during immune activation in mice (Itoh et al., 1996; Nowell et al., 2006). Taken together, it was hypothesized that IL-1α, which acts in the acute-phase response, induces IL-6 and IL-8 via the p38 MAPK pathway and that MT and NAMPT would be upregulated by cytokines such as IL-6.

In the present study, 3 different assays were compared to assess the risk of carboxylic acid-containing drugs. All methods accurately identified the high-risk withdrawn drugs; however, the immunostimulation assay was superior in terms of negative predictive value. This finding suggests that high reactivity does not always have the potential to activate an immune response. The evaluation of immune responses using hPBMCs had the highest accuracy in the present study, but this method requires authentic AG standards. Therefore, this assay is appropriate in the late stages of preclinical drug development.

In conclusion, 3 assay systems were compared to assess the toxicity risk of AGs. The results indicated that the immunostimulation assay is more suitable to evaluate toxicity risk than the assay of half-lives or the formation of peptide adducts. However, the latter 2 assays are more convenient because there is no requirement for authentic AG standards. It is proposed that each assay system can be adopted, depending on the stage in drug development. In early stage, new chemical entities are evaluated using high-throughput assays of half-lives and peptide adducts in the early stages. If the drugs are judged as toxic in both assays, the immunostimulation assay using authentic AGs should be conducted to accurately determine toxicity prior to clinical trials.

CHAPTER 3

In vivo toxicological evaluation of zomepirac acyl glucuronide

SUMMARY

Glucuronidation, an important phase II metabolic route, is generally considered as a detoxification pathway. However, AGs have been implicated in the toxicity of drugs containing carboxyl acid moiety due to their electrophilic reactivity. Zomepirac (ZP) was withdrawn from the market because of their adverse effects such as renal toxicity. ZP is mainly metabolized to acyl glucuronide (ZP-AG) by UGT. However, the responsibility of ZP-AG to renal toxicity has never been proven. In this study, ZP-induced kidney injury mouse model was established by pretreatment with tri-*o*-tolyl phosphate (TOTP), a non-selective esterase inhibitor, and L-buthionine-(*S*,*R*)-sulfoximine (BSO), a glutathione synthesis inhibitor, and then the responsibility of ZP-AG to renal toxicity was investigated. The mouse model showed significant increase in blood urea nitrogen (BUN) and creatinine (CRE), but not increase in alanine aminotransferase. It was demonstrated that the ZP-AG levels were elevated by co-treated with TOTP in the plasma and liver and especially in the kidney. The ZP-AG concentrations in kidney were correlated with BUN and CRE in mice receiving inhibitors and those not receiving inhibitors. In histopathological examination, the vacuoles and infiltration of mononuclear cells were observed in model mouse as described above. In addition to immune- and inflammation-related responses, the oxidative stress markers such as glutathione/disulfide glutathione ratio and malondialdehyde (MDA) levels were changed by TOTP, BSO and ZP-administration. Since the ZP-induced kidney injury was suppressed by treatment with tempol, an antioxidant agent, the involvement of oxidative stress was suggested in the ZP-induced kidney injury. This is the first study to demonstrate that AG accumulation in the kidney by TOTP and BSO-treatment would be a reason of the renal toxicity, and to show the *in vivo* toxicological potential of AGs.

INTRODUCTION

Zomepirac (ZP), a nonsteroidal anti-inflammatory drug, was withdrawn from the market because of their adverse effects such as anaphylaxis and renal toxicity (Smith, 1982; Miller et al., 1983; Heintz, 1995). ZP is mainly metabolized to acyl glucuronide (ZP-AG) in human (Grindel et al., 1980; O'Neill et al., 1982). ZP-AG is more physicochemically unstable in phosphate buffer than the other AGs of safe drugs such as gemfibrozil, repaglunide and telmisartan (Sawamura et al., 2010). ZP-AG also covalently modifies dipeptidyl peptidase IV in rat liver homogenates and microtubular protein in bovine brain *in vitro* (Bailey et al., 1998; Wang et al., 2001). In Chapter 2, it was demonstrated that ZP-AG showed the highest induction of the mRNA expression immune- and inflammation-related genes in hPBMCs in the AGs of 13 drugs. Although the toxicity of ZP-AG has been suggested, there is no evidence that ZP-AG is involved in ZP-induced toxicity *in vivo* in both human and laboratory animals because of the difficulty of the toxicological assessment under the conditions sufficiently exposed to ZP-AG *in vivo*.

The production level of AG is determined by glucuronidation catalyzed by UGT and enzymatic hydrolysis. The enzymatic hydrolysis of AG is catalyzed by esterases such as acylpeptide hydrolase and α/β hydrolase domain containing 10 (Suzuki et al., 2010; Iwamura et al., 2012). It was reported that the plasma clearance of ZP-AG in guinea pig was decreased by phenylmethylsulfonyl fluoride, a general esterase inhibitor, suggesting that ZP-AG is hydrolyzed by esterases (Smith et al., 1990). In other reports, esterases were potently inhibited by TOTP, a non-selective esterase inhibitor, in mice and rats *in vivo* (Silver and Murphy, 1981; Kobayashi et al., 2012). Beside, ZP-AG was known to be conjugated with GSH in rat hepatocytes and bile (Grillo and Hua, 2003). Collectively, the ZP-AG level would be regulated via hydrolysis by esterases and GSH conjugation against the generation by UGT. It is assumed that the increased exposure to ZP-AG *in vivo* by TOTP and BSO after ZP administration may show that ZP-AG rather than ZP is involved in ZP-induced toxicity *in vivo*. The purpose of the present study was to establish the ZP-induced kidney injury mouse model and to investigate

the responsibility of ZP-AG in the kidney injury.

EXPERIMENTAL PROCEDURES

Chemicals and reagents

Reduced GSH, oxidized GSH and BSO were purchased from Wako Pure Chemical Industries. Zomepirac sodium and 4-hydroxy-2,2,6,6-tetramethylpiperidine 1-oxyl (tempol) was obtained from Sigma-Aldrich. ZP-AG and TOTP was purchased from Toronto Research Chemicals and Acros Organics (Morris Plains, NJ), respectively. β-NADPH and GSH reductase were obtained from Oriental Yeast (Tokyo, Japan). A ReverTra Ace qPCR RT kit was obtained from Toyobo (Osaka, Japan). RNAiso Plus and SYBR Premix ExTaq (Tli RNaseH Plus) were obtained from Takara (Otsu, Japan). All primers were commercially synthesized at Hokkaido System Sciences (Sapporo, Japan). Fuji DRI-CHEM slides of GPT/ALT-PIII, BUN-PIII and CRE-PIII, which were used to measure ALT, blood urea nitrogen (BUN) and creatinine (CRE), respectively, were from Fujifilm (Tokyo, Japan). Rabbit polyclonal antibody against myeloperoxidase (MPO) was purchased from DAKO (Carpinteria, CA). A Thiobarbituric Acid Reactive Substances (TBARS) Assay kit was obtained from Oxford Biomedical Research (Oxford, MI). Other chemicals used in this study were of analytical grade or were the highest grade commercially available.

Animals

Nine- to eleven-week-old female BALB/cCrSlc mice were obtained from Japan SLC (Hamamatsu, Japan). The animals were housed under a 12-hlight/dark cycle (lights on 9:00–21:00 h) in a controlled environment (temperature 23 ± 2°C and humidity 55 ± 10%) in the institutional animal facility. All animals were allowed free access to food and water, except when fasting was being conducted. The animals were acclimatized before use in the experiments. All procedures were carried out in accordance with the guidelines established by the Institute for Laboratory Animal Research of the Medical School of Nagoya University.

Administration of ZP, TOTP and BSO

ZP was dissolved in KPB (pH 7.4, 5-15 mg/mL) and intraperitoneally administered to the mice at a dose of 50-150 mg/kg. TOTP was dissolved in corn oil (10 mg/mL) and orally administered at a dose of 50 mg/kg to mice 12 h before the ZP administration. BSO was dissolved in saline (70 mg/mL) and intraperitoneally administered at a dose of 700 mg/kg to mice 1 h before the ZP administration after overnight fasting. The BSO dosage was decided to be 700 mg/kg because this dose has previously decreased GSH level in liver (Shimizu et al., 2009).

Administration of antioxidant agent

Mice were intraperitoneally administered tempol, an antioxidant agent (200 mg/kg in sterilized PBS) at 6 h and 18 h after ZP administration. The plasma was collected at 12 h and 24 h after ZP administration.

ZP and ZP-AG Concentrations in plasma, liver and kidney

Livers and kidneys were homogenized with homogenate buffer consisted of 10 mM Tris-HCl (pH 7.4), 20% glycerol, 1 mM EDTA (pH 8.0). Plasma and tissue concentrations of ZP and ZP-AG were determined by high-performance liquid chromatography (HPLC). Briefly, 5 μL of plasma or 1.25 mg of tissue homogenates were mixed with 20 μL acetonitrile and 35 μL of 8% $HClO_4$ to precipitate the protein. The mixture was centrifuged at 13,000 g for 5 min, and a 40-μL sample of the supernatant was subjected to HPLC. The HPLC analysis was performed using an L-2130 pump (Hitachi), an L-2200 autosampler (Hitachi), an L-2400 UV detector (Hitachi) equipped with a Mightysil RP-18 C18 GP column (5 μm particle size, 4.6 mm i.d. x 150 mm: Kanto Chemical, Tokyo, Japan). The eluent was monitored at 313 nm. Mobile phases were 47% methanol/10 mM acetate buffer (pH 5.0). The quantification of ZP and ZP-AG was performed by comparing the peak areas with those of authentic standards.

Histopathological examination

Kidney samples were fixed in 10% neutral-buffered formalin. The fixed samples were dehydrated with alcohols and embedded in paraffin. Serial sections were stained with hematoxylin-eosin (H&E) for histopathological examination. Neutrophil infiltration was assessed by MPO immunostaining. A rabbit polyclonal antibody against MPO was used for kidney immunohistochemical staining as previously described (Kumada et al., 2004). Two visual fields at a 200-fold magnification (0.2 mm^2 each) were randomly selected from each MPO-immunostained specimen. The average number of MPO-positive cells from two randomly selected visual fields was compared among the specimens.

Real-time RT-PCR

RNA was isolated from livers and kidneys using RNAiso Plus according to the manufacturer's instructions. The mRNA expression of IL-1α, IL-6, macrophage inflammatory protein-2 (MIP-2/CXCL2), intercellular adhesion molecule-1 (ICAM-1/CD54), S100 calcium-binding protein A9 (S100A9), heme oxygenase 1 (HO-1) were quantified using real-time RT-PCR. RT was performed using a ReverTra Ace qRT-PCR kit, according to the manufacturer's instructions. In brief, 1 μg of total RNA was mixed with an appropriate volume of five-fold RT buffer, enzyme mix, primer mix, and nuclease-free water to adjust the total volume to 20 μl, and the RT reaction was carried out at 37°C for 15 min and 98°C for 5 min. Real-time RT-PCR was performed using a Mx3000P (Agilent Technologies, Santa Clara, CA), and the PCR conditions included denaturation at 95°C for 30 s, followed by 40 amplification cycles of 95°C for 5 s and 60°C for all of targets. The amplified products were monitored directly by measuring the increase in the intensity of the SYBR Green I dye binding to the double-stranded DNA amplified by PCR, and a dissociation curve analysis was conducted to confirm the amplification of the PCR product. The sequences of the used primers are shown in Table 8.

Table 8. Sequences of primers used for real-time RT-PCR analyses.

Genes		Primer sequences	NCBI accession No.
IL-1α	S	5'- TTACAGTGAAAACGAAGAC -3'	NM_010554.4
	AS	5'- GATCTGTGCAAGTCTCATGAAG -3'	
IL-6	S	5'- CCATAGCTACCTGGAGTACA -3'	NM_031168.1
	AS	5'- GGAAATTGGGGTAGGAAGGA -3'	
MIP-2	S	5'- AAGTTTGCCTTGACCCTGAAG -3'	NM_009140.2
	AS	5'- ATCAGGTACGATCCAGGCTTC -3'	
ICAM-1	S	5'- GCTACCATCACCGTGTATTCG -3'	NM_010493.2
	AS	5'- TGAGGTCCTTGCCTACTTGC -3'	
S100A9	S	5'- GATGGCCAACAAAGCACCTT -3'	NM_009114.3
	AS	5'- CCTCAAAGCTCAGCTGATTG -3'	
HO-1	S	5'- GACACCTGAGGTCAAGCACA -3'	NM_010442.2
	AS	5'- ATCACCTGCAGCTCCTCAAA -3'	

S, Sense; AS, Anti-sense.
IL, interleukin; MIP-2, macrophage inflammatory protein-2; ICAM-1, intercellular adhesion molecule-1; S100A9, S100 calcium-binding protein A9; HO-1, heme oxygenase 1.

GSH levels in kidney and liver

Livers and kidneys were homogenized with ice-cold 5% sulfosalicylic acid and centrifuged at 8,000 g for 10 min at 4°C. The supernatant was collected, and the total GSH and disulfide glutathione (GSSG) concentrations were measured as previously described (Tietze, 1969; Griffith, 1980). The reduced GSH contents were calculated from the total GSH and the GSSG contents.

Malondialdehyde (MDA) levels in kidney and liver

Livers and kidneys were homogenized with homogenate buffer. A half volume of trichloroacetic acid (1 g/mL) was added to tissue homogenates to precipitate proteins and acidify the samples, and centrifuged at 12,000 g for 5 min at 4°C. The supernatant was collected, and the MDA concentrations were measured using a TBARS Assay kit (Oxford Biomedical Research) according to the manufacturer's protocol. The TBARS was detected by fluorescence (excitation 532 nm, emission 585 nm) using a PowerScan4 (DS Pharma Biomedical, Osaka, Japan).

Statistical analysis

The statistical analysis of multiple groups was performed using Dunnett's test or Tukey's test to determine the significance of differences between individual groups. Comparisons between two groups were carried out using two-tailed Student's *t*-tests. A value of $P < 0.05$ was considered statistically significant.

RESULTS

Establishment of the ZP-induced kidney injury mouse model

In female BALB/c mice administrated with ZP (150 mg/kg, i.p.), the plasma levels of CRE, BUN and ALT were not increased at 24 h after the administration (Fig. 8). Considering the possibility that GSH conjugation and hydrolysis of ZP-AG might be involved in ZP-induced toxicity, the effects of co-treatment with BSO or TOTP, a GSH synthesis inhibitor (Shimizu et al., 2009) or an esterase inhibitor (Emeigh Hart et al., 1991), respectively, were investigated. Co-administration of BSO resulted in slight increase in CRE and BUN compared with the group administered with ZP alone. Whereas, CRE and BUN were significantly elevated by co-administration of TOTP, although ALT was not affected. The highest increases in CRE and BUN were observed in mice co-administrated with both TOTP and BSO. No increase in plasma CRE, BUN and ALT levels in mice receiving TOTP or BSO only was confirmed. These results suggest that the inhibition of GSH conjugation and hydrolysis of ZP-AG contributes to the kidney injury caused by ZP administration.

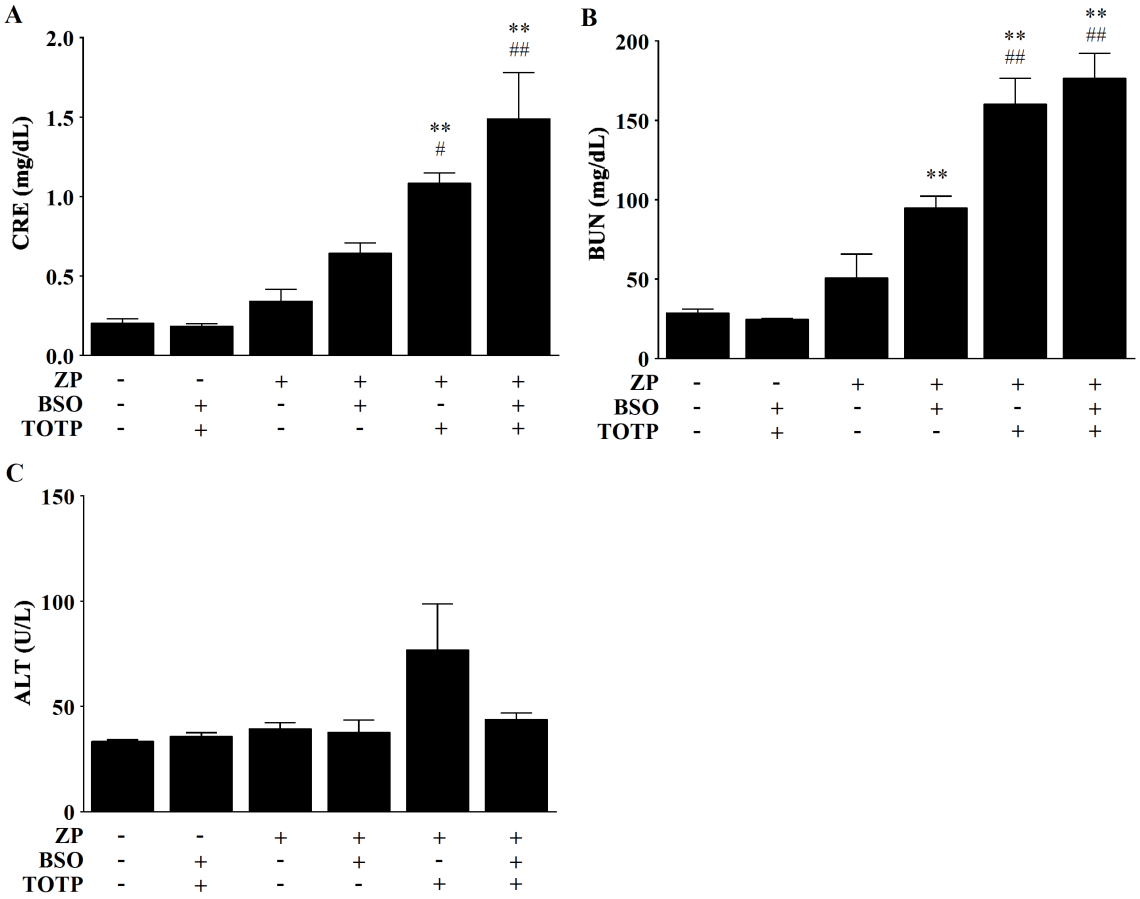

Fig. 8. Changes in plasma CRE (A), BUN (B) and ALT (C) levels in female BALB/c mice after ZP administration. TOTP (50 mg/kg in corn oil, p.o.), BSO (700 mg/kg in saline, i.p.) and ZP (150 mg/kg in KPB, i.p.) were administered as described in Experimental Procedures. The plasma CRE, BUN and ALT levels were measured 24 h after ZP administration. The data are shown as the mean ± SEM (n = 5-7). The statistical analyses were performed using one-way ANOVA followed by Dunnett's test. $^{**}P < 0.01$ compared with the vehicles (corn oil, saline and KPB) alone-treated group. $\#P < 0.05$, $\#\#P < 0.01$ compared with the ZP alone-treated group.

Dose- and time-dependent changes of ZP-induced kidney injury

ZP was administered at a dose of 50, 100, or 150 mg/kg with co-administration of TOTP and BSO to mice. Plasma CRE and BUN levels were significantly and dose-dependently increased in mice receiving 100 and 150 mg/kg of ZP compared with vehicle (KPB)-administered control mice; thus for subsequent experiments we adapted a dose of ZP at 150 mg/kg (Fig. 9). As shown in Figs. 10A-10C, plasma CRE and BUN levels were time-dependently increased 12 and 24 h after ZP-administration, but plasma ALT levels did not.

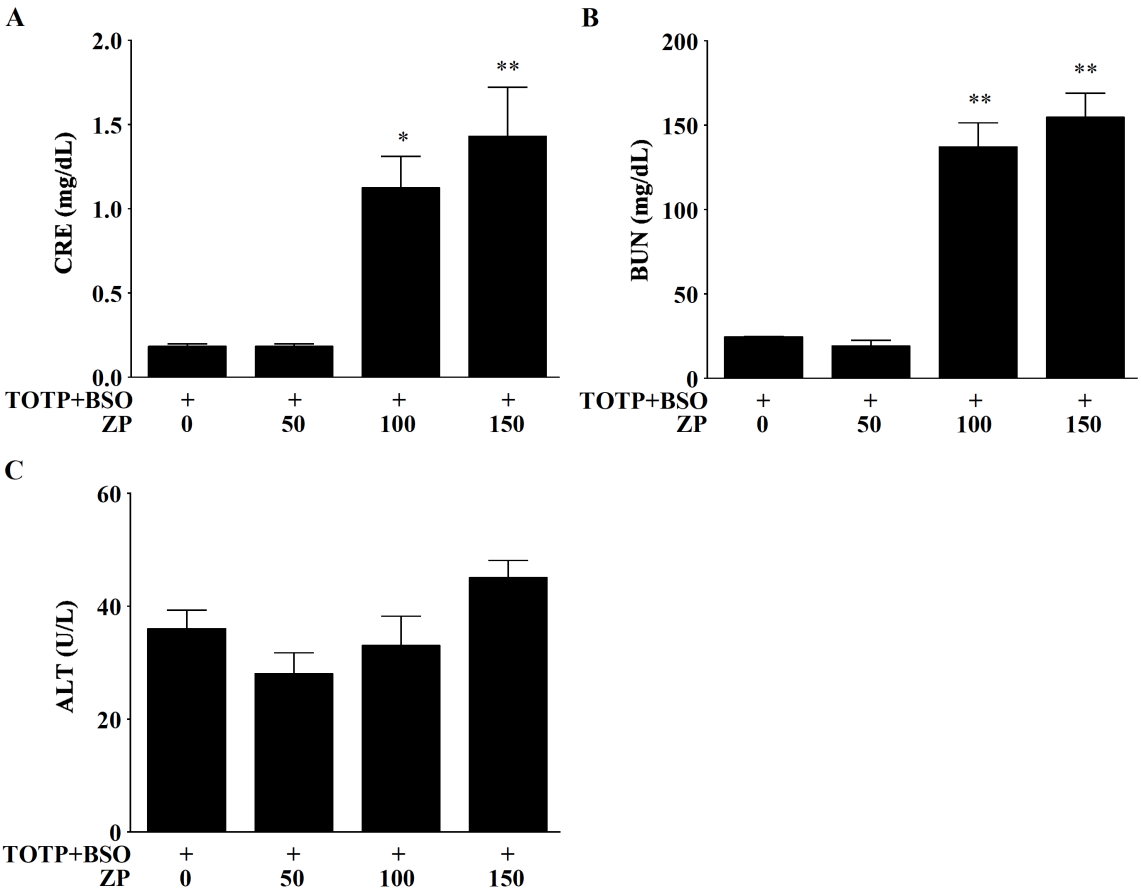

Fig. 9. Dose-dependent changes in plasma CRE (A), BUN (B) and ALT (C) levels after ZP administration in mice. TOTP and BSO were administered as described in Experimental Procedures. ZP was administered at a dose of 50, 100 and 150 mg/kg. The plasma CRE, BUN and ALT levels were measured 24 h after ZP administration. The data are shown as the mean ± SEM (n = 5-7). Differences compared with the inhibitors alone-treated group were considered significant at $*P < 0.05$, $**P < 0.01$ by one-way ANOVA followed by Dunnett's test.

Time-dependent changes of ZP and ZP-AG concentrations in plasma, kidney and liver

The concentrations of ZP and ZP-AG in plasma, kidney and liver were measured in mice after ZP administration with or without co-administration of TOTP and BSO. In plasma, kidney and liver, the concentrations of ZP were significantly lower in mice receiving TOTP, BSO and ZP compared with those in mice receiving ZP alone (Fig. 10D). Whereas, the plasma and the tissue concentrations of ZP-AG were significantly higher in mice receiving TOTP, BSO and ZP compared with those in mice receiving ZP alone (Fig. 10E). In groups co-administered with or without the inhibitors, the ZP concentrations in the kidney were almost the same as those in the liver, whereas the ZP-AG concentrations in the kidney were much higher than those in the liver. These results imply that the ZP-AG would slowly be eliminated from the kidney, resulting in high accumulation in the kidney.

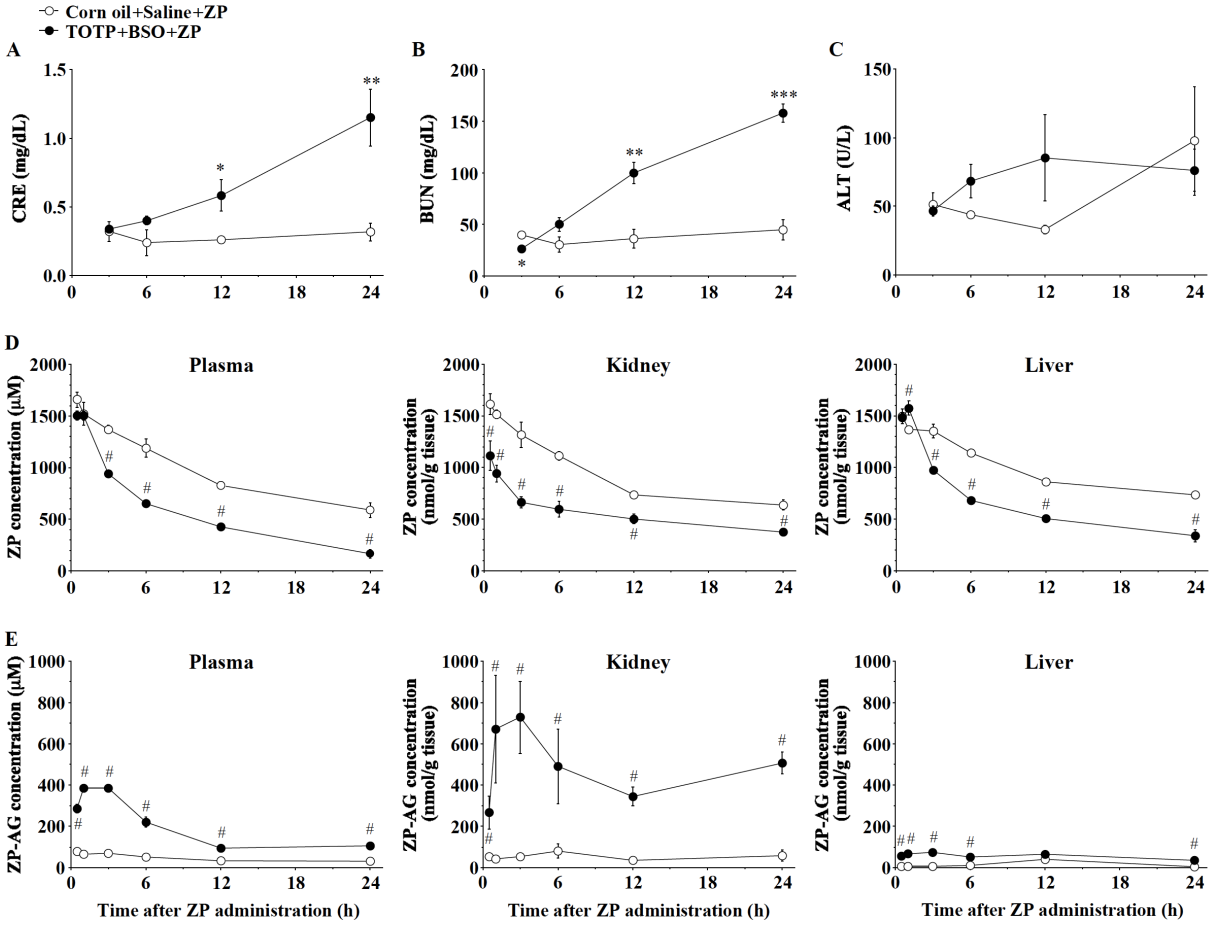

Fig. 10. Time-dependent changes in plasma CRE (A), BUN (B), ALT (C) levels and concentrations of ZP (D) and ZP-AG (E) in plasma, kidney and liver after ZP administration. TOTP, BSO and ZP were administered as described in Experimental Procedures. The plasma CRE, BUN and ALT levels were measured 3, 6, 12 and 24 h after ZP administration. Concentrations of ZP and ZP-AG in plasma, kidney and liver were measured 0.5, 1, 3, 6, 12 and 24 h after ZP administration. The data are shown as the mean ± SEM (n = 5-7). Differences in plasma CRE, BUN and ALT levels compared with the ZP alone-treated group were considered significant at $*P < 0.05$, $**P < 0.01$, $***P < 0.001$ by Student's *t*-tests. Differences in the concentrations of ZP and ZP-AG in plasma, kidney and liver compared with the ZP alone-treated group were considered significant at $\#P < 0.05$ by Student's *t*-tests.

Histopathological examination in ZP-induced kidney injury

To evaluate the tissue injury, histopathological examination of kidney 24 h after ZP administration (150 mg/kg) was performed. Vacuoles, the denaturation and aggregation of eosinophilic materials were observed in the kidney of mice co-administrated with ZP and inhibitors, although the histological abnormality was mild in mice receiving only ZP, and no abnormality was observed in mice receiving vehicles or only inhibitors (Fig. 11A). In the anti-MPO antibody staining, the number of MPO-positive cells was significantly higher in mice receiving TOTP, BSO and ZP compared to mice receiving only ZP. In contrast, infiltration of mononuclear cells into the renal cells was not observed in mice receiving vehicles- and only inhibitors (Figs. 11B and 11C).

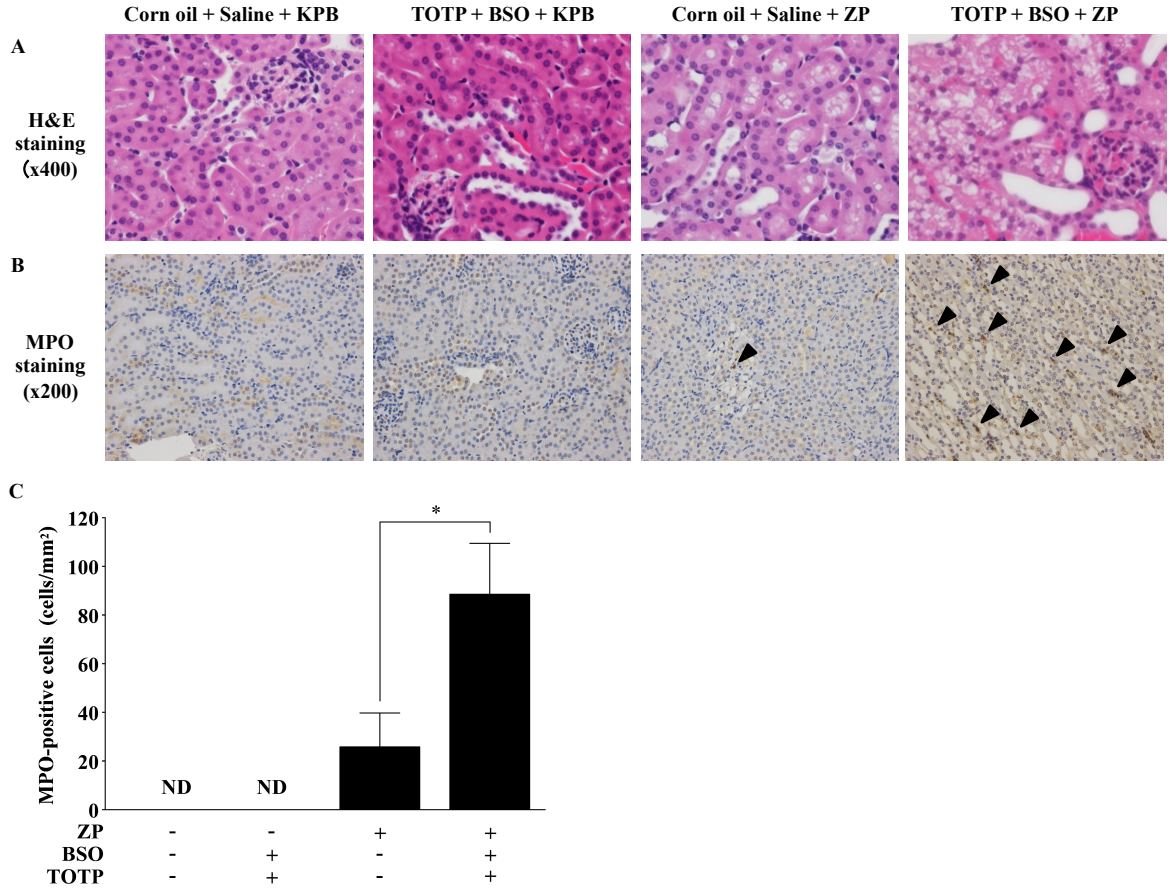

Fig. 11. Histopathological examination of mouse kidney after ZP administration. TOTP, BSO and ZP were administered as described in Experimental Procedures. The kidneys were collected at 24 h after ZP administration, and the kidney sections were stained with hematoxylin and eosin (H&E) (A) or immunostained with an anti-myeloperoxidase (MPO) antibody (B). Arrowheads indicate immune cell infiltration. The number of MPO-positive cells was counted and compared with the ZP alone-treated group (C). The data are shown as the mean ± SEM (n = 5-7). The difference compared between the ZP alone-treated group and ZP and inhibitors-treated group was considered significant at $*P < 0.05$ by Student's *t*-tests.

Changes in mRNA expression levels of immune-, inflammation- and oxidative stress-related genes in kidney

To investigate whether immune-, inflammation- and oxidative stress-related factors are involved in ZP-induced kidney injury, time-dependent changes in the renal mRNA expression levels of IL-1α, IL-6, MIP-2, ICAM-1, S100A9 and HO-1 were measured (Fig. 12). IL-1α mRNA expression levels in only ZP-receiving mice were significantly increased 12 h after ZP administration, and those in TOTP, BSO and ZP-receiving mice were additionally increased not only 12 h but also 1 h after ZP administration. IL-6 and ICAM-1 mRNA expression levels in mice receiving TOTP, BSO and ZP were significantly increased in mice receiving TOTP, BSO and ZP 1 h and 12 h after ZP administration, in contrast to small increase in mice receiving only ZP. S100A9 mRNA expression levels in only ZP-receiving mice were significantly increased 1 h after ZP administration, but those in TOTP, BSO and ZP-receiving mice were significantly increased 12 h and 24 h after ZP administration. Only in mice receiving TOTP, BSO and ZP, the mRNA expression levels of HO-1 were significantly increased 12 h and 24 h after ZP administration. Although the mRNA expression levels of transcription factors for the Th lineage in adaptive immunity, such as T-box expressed in T cells, GATA-binding domain-3 retinoid-related orphan receptor-γt and forkhead box P3, no change was observed in their expressions between any groups (data not shown).

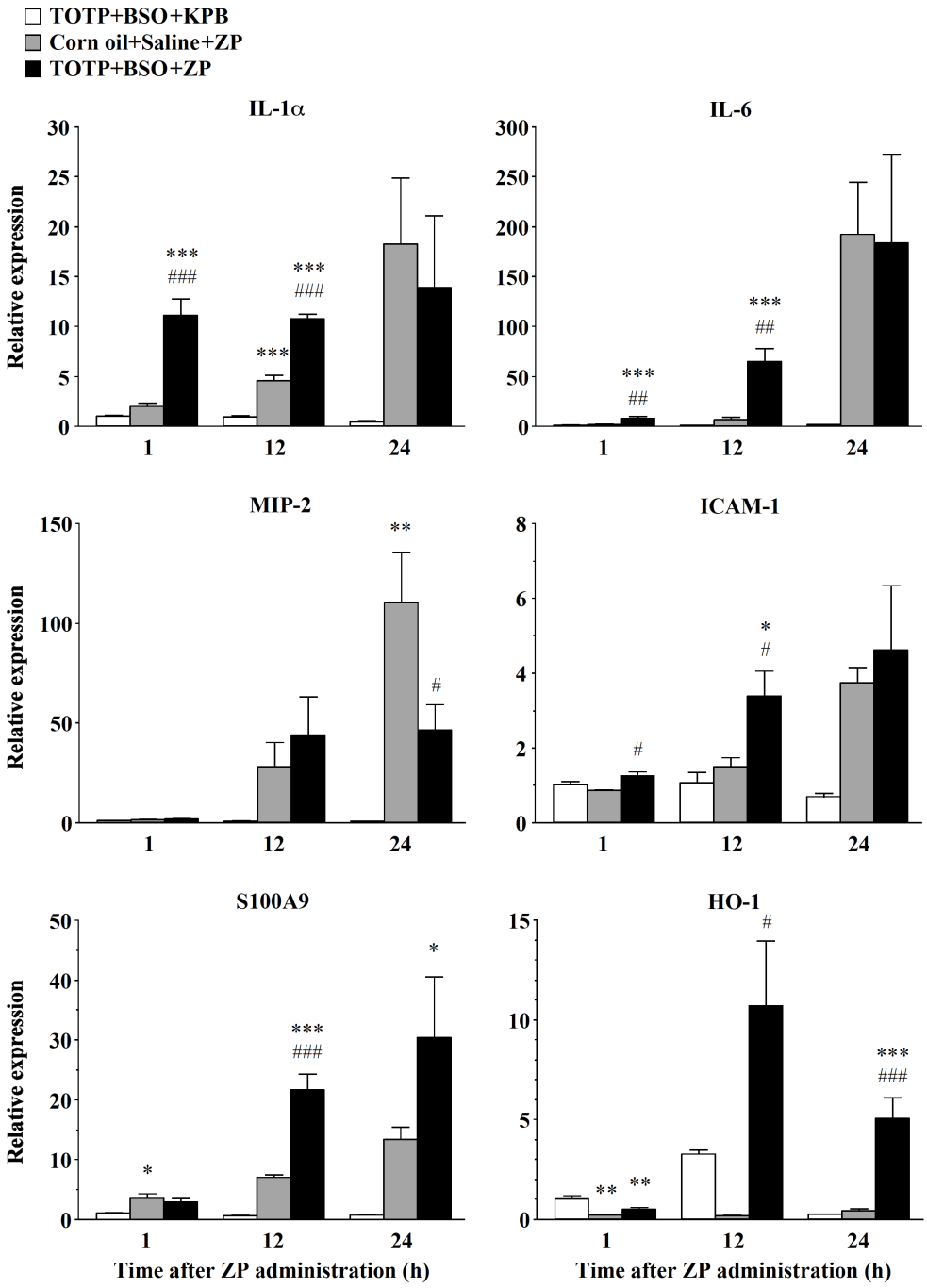

Fig. 12. Time-dependent changes in the renal mRNA expression levels of immune-, inflammation- and oxidative stress-related genes in mice after ZP administration. TOTP, BSO and ZP were administered as described in Experimental Procedures. The kidneys were collected at 1, 12 and 24 h after ZP administration. The expression level of each mRNA was measured by real-time RT-PCR and normalized with that of Gapdh mRNA as described in Experimental Procedures. The data are shown as the mean ± SEM (n = 5-6). The statistical analyses were performed using one-way ANOVA followed by Tukey's test. *$P < 0.05$, **$P < 0.01$, ***$P < 0.001$, compared with the inhibitors alone-treated group. #$P < 0.05$, ##$P < 0.01$, ###$P < 0.001$, compared with the ZP alone-treated group.

Involvement of oxidative stress in ZP-induced kidney injury

To conform the depletion of GSH by BSO treatment and to investigate the involvement of oxidative stress in ZP-induced kidney injury, GSH and GSSG contents in kidney and liver were measured (Figs. 13A-13C). In the kidney, GSH depletion by BSO was conformed in mice treated with TOTP and BSO. In addition, GSH levels in mice receiving TOTP, BSO and ZP were significantly lower compared with those in mice receiving only inhibitors. Owing to the decrease of GSH levels, GSH/GSSG ratio, a biomarker of oxidative stress, was significantly lower in BSO, TOTP and ZP-treated mice compared with BSO and TOTP-treated mice. In liver, GSH was depleted by BSO, but GSH/GSSH ratio was not different between TOTP and BSO-treated group and TOTP, BSO and ZP-treated groups.

In addition, MDA concentrations, a biomarker of lipid peroxidation, were measured in the kidney and liver (Fig. 13D). In the kidney, MDA concentrations were significantly higher in TOTP, BSO and ZP-treated mice compared with TOTP and BSO-treated mice, but in the liver, there was no change in MDA concentrations between these groups.

Effect of an antioxidant agent on ZP-induced kidney injury

The changes of oxidative stress markers implied the involvement of oxidative stress in ZP-induced kidney injury. Next, the effect of tempol, an antioxidant agent, on ZP-induced kidney injury was investigated. The co-administration of tempol significantly decreased the plasma CRE levels at 12 h and BUN levels at 12 and 24 h after ZP administration in BSO, TOTP and ZP-treated mice (Fig. 14). These results also support the involvement of oxidative stress in ZP-induced kidney injury.

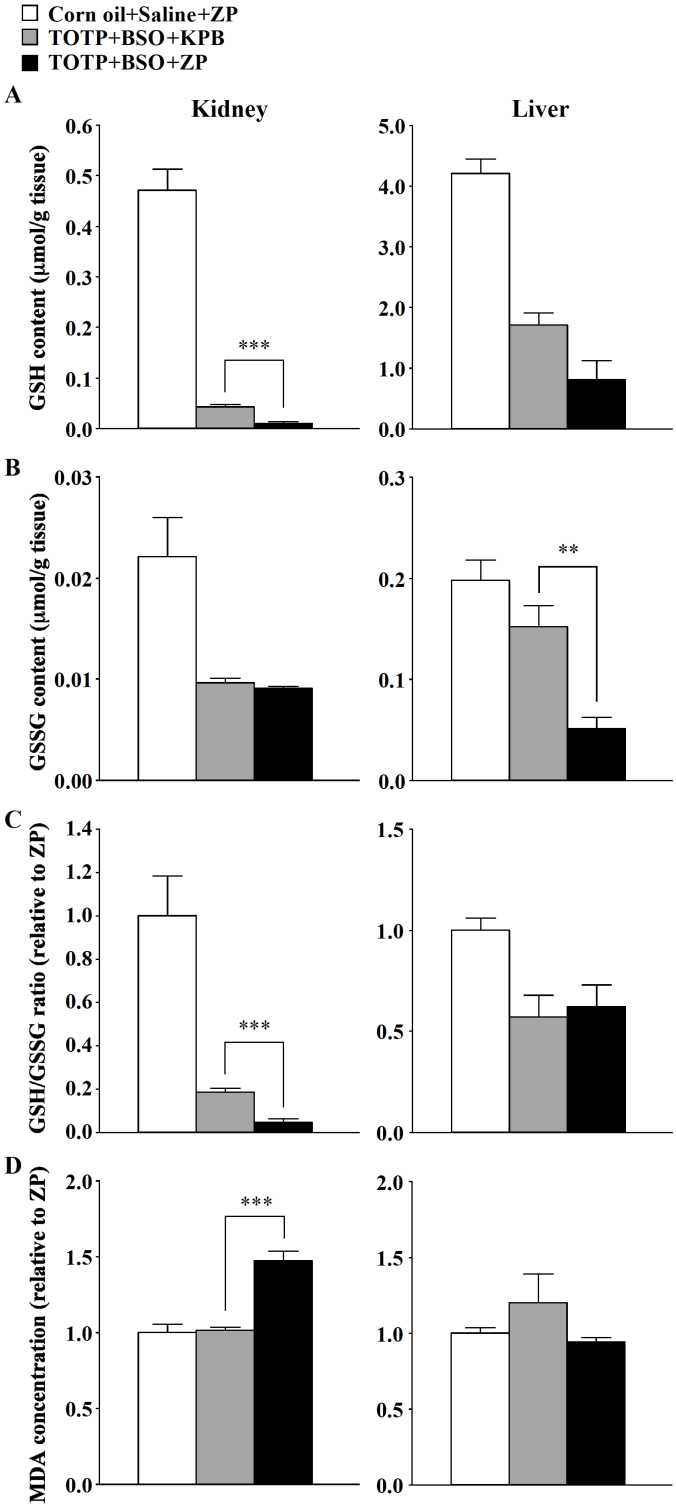

Fig. 13. The GSH (A) and GSSG (B) levels, GSH/GSSG ratio (C) and MDA levels (D) in kidney and liver after ZP administration. TOTP, BSO and ZP were administered as described in Experimental Procedures. The kidney and liver were collected at 12 h after ZP administration. The data are shown as the mean ± SEM (n = 5-6). The difference compared between the inhibitors alone-treated group and ZP and inhibitors-treated group was considered significant at $^{**}P < 0.01$, $^{***}P < 0.001$ by Student's *t*-tests.

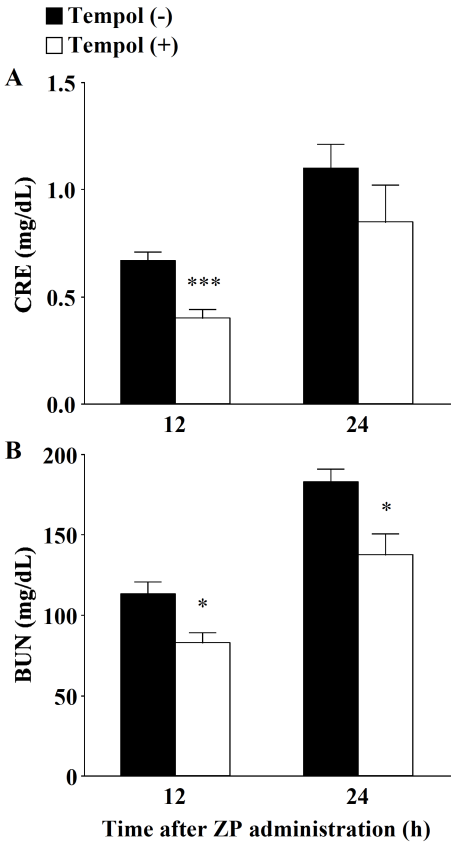

Fig. 14. Effect of an antioxidant agent on kidney injury of ZP-administered mice. TOTP, BSO, ZP and tempol were administered as described in Experimental Procedures. The plasma CRE (A) and BUN (B) levels were measured 12 and 24 h after ZP administration. The data are shown as the mean ± SEM (n = 6). Differences compared with no tempol-treated group were considered significant at $*P < 0.05$, $***P < 0.001$ by Student's *t*-tests.

DISCUSSION

AGs of drugs are generally unstable and are believed to be involved in drug-induced toxicity via the formation of covalent adducts to endogenous proteins. Although there is increasing evidence that AGs form drug-protein adducts owing to their chemical reactivity (Wang et al., 2001; Horng and Benet, 2013), cytotoxicity and genotoxicity of AGs have not been observed in in vitro assays (Koga et al., 2011). In the previous report and Chapter 2, the AGs of warning and withdrawn drugs such as zomepirac and diclofenac induced the mRNA expression levels of immune- and inflammation-related genes in hPBMCs (Miyashita et al., 2014). Thus, the toxicity of AGs evaluated by *in vitro* studies remains controversial.

ZP is a nonsteroidal anti-inflammatory drug that is withdrawn from the market because of severe adverse effects such as anaphylaxis and renal toxicity (Smith, 1982; Miller et al., 1983; Heintz, 1995). It has been shown that ZP-AG, a glucuronide of ZP, covalently bound proteins such as microtubular protein and dipeptidyl peptidase IV in *in vitro* and *in vivo* experiment, suggesting the involvement of ZP-AG in ZP-induced toxicity (Bailey et al., 1998; Wang et al., 2001). However, an animal model for the toxicity induced by ZP-AG has never been reported. In order to establish a mouse model of the toxicity induced by ZP-AG, we attempted to increase the exposure of ZP-AG in mice by inhibiting its hydrolysis by using an inhibitor of esterases. A previous study reported that ZP-AG is hydrolyzed by esterases (Smith et al., 1990). TOTP, a non-selective esterase inhibitor, successfully inhibited esterase activity in mice and rats *in vivo* (Silver and Murphy, 1981; Kobayashi et al., 2012). In the present study, in addition to TOTP, BSO was used to reduce the GSH conjugation of ZP-AG.

The renal and hepatic toxicity was not observed by administration of only ZP. Co-administration of TOTP significantly increased the plasma CRE and BUN levels and that of BSO moderately increased them. Co-administration of TOTP and BSO with ZP showed the severest renal toxicity, suggesting that hydrolysis and GSH conjugation of ZP-AG have a role for detoxification of ZP-AG. In contrast to plasma CRE and BUN levels, plasma ALT levels were not elevated in any groups, which corresponds to the facts that acute kidney injury was

frequently reported in ZP therapy in human. The present study succeeded to establish an animal model of ZP-induced kidney injury by co-administration of TOTP and BSO.

To examine the relationship between the extent of kidney injury and the exposure of ZP and ZP-AG, the concentrations of ZP and ZP-AG in the plasma, kidney and liver were measured. ZP-AG concentrations in plasma, kidney and liver were significantly higher in mice receiving TOTP, BSO and ZP compared with in mice receiving ZP alone. Especially high concentration of ZP-AG was observed in the kidney, suggesting ZP-AG had potential to lead to kidney injury. ZP-AG concentrations in the liver were much lower than those in the kidney, although the ZP concentrations in the liver were almost the same as those in the kidney. These results indicated that ZP-AG was more toxic than ZP, because no hepatotoxicity was observed after ZP dosing. ZP and its metabolites are primarily excreted into urine, and urinary principal metabolite is ZP-AG in both mouse and human, whereas the urinary excretion ratio of ZP-AG in human is higher than that in mouse (57% and 19-28% of dose, respectively) (Grindel et al., 1980). Therefore, the exposure level of ZP-AG in the present model mouse receiving inhibitors, rather than normal mouse, would be close to that in human, suggesting that this model might be used to predict the toxicity caused by ZP-AG in human.

In general, glucuronides in hepatocytes are eliminated into bile and blood by multidrug-resistance protein (Mrp) 2 and Mrp 3, respectively (Trauner and Boyer, 2003). It has been demonstrated that, in human hepatocytes, the AGs of NSAIDs (diclofenac, naproxen, ketoprofen and ibuprofen) were rapidly excreted and did not accumulate in the cell (Koga et al., 2011). ZP-AG would be immediately exported from liver into blood rather than bile, because excretion of ZP and its metabolites into bile is a minor route in human and laboratory animals (Grindel et al., 1980). Thus, these reports support the finding that ZP-AG accumulated in the kidney, but not in the liver.

In histopathological examination, the present mouse model of ZP-induced kidney injury displayed vacuoles and denatured cytoplasm and aggregated eosinophilic materials, probably reflecting cellular necrosis. In the ZP-induced kidney injury in clinical, renal cortical necrosis was observed (Darwish et al., 1984), and the results observed in the present study was

consistent with the clinical findings. In preclinical studies, almost all of the NSAIDs produced papillary necrosis in experimental animal models (Whelton and Hamilton, 1991). The possible mechanism of papillary necrosis is ischemic injury through the direct inhibition of cyclooxygenase-mediated production of prostaglandins (Brix, 2002). However, the inhibition of cyclooxygenase by ZP might not contribute to ZP-induced kidney injury because papillary necrosis was not observed in this injury. The increased number of MPO-positive cells suggested the contribution of immune cell infiltration to ZP-induced kidney injury.

From the results in Chapter 2, AGs of warning and withdrawn drugs induced immune- and inflammation-related genes such as IL-1α and IL-6 in hPBMCs. Hence, the changes in the renal mRNA expression levels of immune- and inflammation-related genes were measured. The mRNA expressions of IL-1α and IL-6 were induced in the mice highly exposed to ZP-AG, and followed by ICAM-1 and S100A9 mRNAs. IL-1α, a trigger of cascades of chemokines, other cytokines and inflammatory mediators, is synthesized in the first few hours in the injurious or ischemic event (Dinarello et al., 2012). IL-6 is also rapidly induced as a lymphocyte-stimulating factor and leads to innate and adaptive immune activation (Hunter and Jones, 2015). ICAM-1, an adhesion molecule, is involved in infiltration of inflammatory cells (Ley et al., 2007). S100A9, damage-associated molecular patterns, is released from activated or necrotic neutrophils and monocytes/macrophages and promotes innate immune and inflammation (Schiopu and Cotoi, 2013). The stimulation of IL-1α induces ICAM-1 and S100A9 (Aziz and Wakefield, 1996; Zreiqat et al., 2010), and so does IL-6 (Wung et al., 2005; Lee et al., 2012). Because the injection of recombinant IL-1α accelerates renal injury and mortality in mice (Brennan et al., 1989), and IL-6- or ICAM-1-deficient mice show protective effect against acute kidney injury, these factors could trigger and promote the kidney injury (Kelly et al., 1996; Nechemia-Arbely et al., 2008). Taken together, it was conceivable that IL-1α and IL-6 induced by ZP-AG at the onset promoted the infiltration of immune cells via the induction of ICAM-1 and MIP-2, and then the infiltrating cells caused kidney injury.

Of particular note was the potent induction of HO-1 mRNA in mice co-administered with TOTP and BSO, suggesting that ZP-AG was involved in ZP-induced kidney injury via the

induction of oxidative stress. The decrease in GSH/GSSG ratio and the increase in MDA concentrations were observed in the kidney, but not in the iver, being consistent with each tissue injury. Partial involvement of oxidative stress was also demonstrated by experiments using tempol. In accordance with the results of the GSH/GSSG ratio and the MDA concentrations, an antioxidant tempol suppressed ZP-induced kidney injury, suggesting that oxidative stress was involved in the renal toxicity. It was reported that the decrease in the GSH/GSSG ratio and the increase in the MDA concentrations were observed in cisplatin-induced acute renal failure in rats (Santos et al., 2007). Tempol attenuated oxidative stress-mediated renal injury in rats (Chatterjee et al., 2000). These results were close to the results observed in the present study.

In conclusion, a mouse model for ZP-induced kidney injury was established by using TOTP and BSO in consideration of the metabolic pathway of ZP. From the pharmacokinetics of ZP and ZP-AG, it was shown that the hydrolysis of ZP-AG by esterases considerably contributed to their pharmacokinetics and ZP-AG would be responsible for ZP-induced kidney injury *in vivo*. In addition, it was demonstrated that the renal toxicity was mediated via oxidative stress and immune cells infiltration. The model using TOTP can be used to evaluate the toxicity of AGs in preclinical, and the present study sheds light on understanding the toxicological potential of AGs.

CHAPTER 4

Conclusion

Highlights in the present study were described as follow.

- Immunostimulation assay using 5 gene expressions in hPBMC as biomarkers showed high accuracy.
- ZP-AG is responsible for ZP-induced kidney injury *in vivo*.
- The evaluation of AG toxicity can contribute to improve the risk assessment in drug development.

AGs covalently bind to endogenous proteins owing to their instability, and have been believed to be related with the toxicity of carboxyl acid drugs. However, the theory remains controversial. The purpose of this study was to evaluate the toxicological potential of AGs by *in vitro* and *in vivo* experiments.

To investigate direct and immune-mediated toxicity by AGs as possible mechanisms of toxicity, in **Chapter 2**, the assays of half-lives, peptide adducts and immunostimulation of AGs of 21 drugs were performed, and then the relationship to the toxic category was analyzed. In half-lives and peptide adducts assays, the AGs of withdrawn drugs had short half-lives and formed glycation adducts, but the AGs of several safe drugs also did. The results indicated that these assays have potential for the false-positive prediction. The stimulation of immune-related factors by AGs was investigated using hPBMCs. The induction of IL-8 mRNA expression by AGs of withdrawn and warning drugs was observed, while that by AGs of safe drugs was not. DNA microarray analysis was performed to search other biomarkers for toxicity of AGs. As the results, in addition to IL-8, 4 genes (IL-1α, IL-6, MT2A, and NAMPT) were found, and an integrated score of the relative expression levels of mRNA of these 5 genes in hPBMCs could successfully distinguish the withdrawn and warning drugs from safe drugs. The immunostimulation assay showed the highest accuracy among three assays tested in this

study, although this assay requires authentic AG standards. In preclinical stage in drug development, the evaluation of immunostimulation by AGs using hPBMCs can contribute to improved drug safety.

ZP was withdrawn from the market due to adverse effects such as renal toxicity and anaphylaxis. It was demonstrated by previous studies that ZP-AG formed protein adducts and the study in Chapter 2 revealed that ZP-AG had the highest total sum score among the tested AGs. However, the toxicity of ZP-AG has not been proved by *in vivo* study. In **Chapter 3**, it was investigated by *in vivo* study whether ZP-AG is responsible for renal toxicity by ZP. No renal toxicity was observed by administration of only ZP, whereas the severe renal toxicity was observed by co-administration of TOTP and BSO with ZP. Co-administration with TOTP and BSO increased concentrations of ZP-AG in plasma and liver, especially in kidney, suggesting that ZP-AG leads to renal toxicity. In the mouse model of ZP-induced kidney injury, MPO-positive cells infiltrated into the renal cells; hence, the mRNA expression levels of immune- and inflammation-related genes were measured. In addition to ICAM-1 that is involved in immune cell infiltration, IL-1α, IL-6 and S100A9 mRNA expression were induced in the mouse model. The mRNA expression levels of HO-1, an oxidative stress-related gene, were also increased. In accordance with these results, GSH/GSSG ratio was decreased and MDA level was increased in kidney. In addition, an antioxidant agent, tempol attenuated ZP-induced kidney injury. The mouse model established in the present study is expected to be used for evaluating the *in vivo* toxicity of AGs in preclinical stage in drug development.

In conclusion, this study provides new insight into the evaluation of AG toxicity in drug development.

REFERENCES

Aziz KE and Wakefield D (1996) Modulation of endothelial cell expression of ICAM-1, E-selectin, and VCAM-1 by beta-estradiol, progesterone, and dexamethasone. *Cell Immunol* **167:**79-85.

Baggiolini M, Dewald B, and Moser B (1994) Interleukin-8 and related chemotactic cytokines--CXC and CC chemokines. *Adv Immunol* **55:**97-179.

Bailey MJ and Dickinson RG (2003) Acyl glucuronide reactivity in perspective: biological consequences. *Chem Biol Interact* **145:**117-137.

Bailey MJ, Worrall S, de Jersey J, and Dickinson RG (1998) Zomepirac acyl glucuronide covalently modifies tubulin in vitro and in vivo and inhibits its assembly in an in vitro system. *Chem Biol Interact* **115:**153-166.

Benet LZ, Spahn-Langguth H, Iwakawa S, Volland C, Mizuma T, Mayer S, Mutschler E, and Lin ET (1993) Predictability of the covalent binding of acidic drugs in man. *Life Sci* **53:**PL141-146.

Boelsterli UA (2002) Xenobiotic acyl glucuronides and acyl CoA thioesters as protein-reactive metabolites with the potential to cause idiosyncratic drug reactions. *Curr Drug Metab* **3:**439-450.

Brennan DC, Yui MA, Wuthrich RP, and Kelley VE (1989) Tumor necrosis factor and IL-1 in New Zealand Black/White mice. Enhanced gene expression and acceleration of renal injury. *J Immunol* **143:**3470-3475.

Brix AE (2002) Renal papillary necrosis. *Toxicol Pathol* **30:**672-674.

Chatterjee PK, Cuzzocrea S, Brown PA, Zacharowski K, Stewart KN, Mota-Filipe H, and Thiemermann C (2000) Tempol, a membrane-permeable radical scavenger, reduces oxidant stress-mediated renal dysfunction and injury in the rat. *Kidney Int* **58:**658-673.

Chen Z, Holt TG, Pivnichny JV, and Leung K (2007) A simple in vitro model to study the stability of acylglucuronides. *J Pharmacol Toxicol Methods* **55:**91-95.

Darwish R, Vaziri ND, Gupta S, Novey H, Spear GS, Licorish K, Powers D, and Cesario T

(1984) Focal renal cortical necrosis associated with zomepirac. *Am J Med* **76:**1113-1117.

Dinarello CA, Simon A, and van der Meer JW (2012) Treating inflammation by blocking interleukin-1 in a broad spectrum of diseases. *Nat Rev Drug Discov* **11:**633-652.

Emeigh Hart SG, Beierschmitt WP, Bartolone JB, Wyand DS, Khairallah EA, and Cohen SD (1991) Evidence against deacetylation and for cytochrome P450-mediated activation in acetaminophen-induced nephrotoxicity in the CD-1 mouse. *Toxicol Appl Pharmacol* **107:**1-15.

Faed EM (1984) Properties of acyl glucuronides: implications for studies of the pharmacokinetics and metabolism of acidic drugs. *Drug Metab Rev* **15:**1213-1249.

Garlanda C, Dinarello CA, and Mantovani A (2013) The interleukin-1 family: back to the future. *Immunity* **39:**1003-1018.

Griffith OW (1980) Determination of glutathione and glutathione disulfide using glutathione reductase and 2-vinylpyridine. *Anal Biochem* **106:**207-212.

Grillo MP and Hua F (2003) Identification of zomepirac-S-acyl-glutathione in vitro in incubations with rat hepatocytes and in vivo in rat bile. *Drug Metab Dispos* **31:**1429-1436.

Grindel JM, O'Neill PJ, Yorgey KA, Schwartz MH, McKown LA, Migdalof BH, and Wu WN (1980) The metabolism of zomepirac sodium. I. Disposition in laboratory animals and man. *Drug Metab Dispos* **8:**343-348.

Grubb N, Weil A, and Caldwell J (1993) Studies on the *in vitro* reactivity of clofibryl and fenofibryl glucuronides. Evidence for protein binding via a Schiff's base mechanism. *Biochem Pharmacol* **46:**357-364.

Haynes V, Connor T, Tchernof A, Vidal H, and Dubois S (2013) Metallothionein 2a gene expression is increased in subcutaneous adipose tissue of type 2 diabetic patients. *Mol Genet Metab* **108:**90-94.

Heintz RC (1995) Tenoxicam and renal function. *Drug Saf* **12:**110-119.

Hirano T and Kishimoto T (1989) Interleukin-6: possible implications in human diseases. *Ric*

Clin Lab **19:**1-10.

Horng H and Benet LZ (2013) The nonenzymatic reactivity of the acyl-linked metabolites of mefenamic acid toward amino and thiol functional group bionucleophiles. *Drug Metab Dispos* **41:**1923-1933.

Hunter CA and Jones SA (2015) IL-6 as a keystone cytokine in health and disease. *Nat Immunol* **16:**448-457.

Islam Z, Gray JS, and Pestka JJ (2006) p38 Mitogen-activated protein kinase mediates IL-8 induction by the ribotoxin deoxynivalenol in human monocytes. *Toxicol Appl Pharmacol* **213:**235-244.

Itoh N, Kasutani K, Muto N, Otaki N, Kimura M, and Tanaka K (1996) Blocking effect of anti-mouse interleukin-6 monoclonal antibody and glucocorticoid receptor antagonist, RU38486, on metallothionein-inducing activity of serum from lipopolysaccharide-treated mice. *Toxicology* **112:**29-36.

Iwamura A, Fukami T, Higuchi R, Nakajima M, and Yokoi T (2012) Human α/β hydrolase domain containing 10 (ABHD10) is responsible enzyme for deglucuronidation of mycophenolic acid acyl-glucuronide in liver. *J Biol Chem* **287:**9240-9249.

Jinno N, Ohashi S, Tagashira M, Kohira T, and Yamada S (2013) A simple method to evaluate reactivity of acylglucuronides optimized for early stage drug discovery. *Biol Pharm Bull* **36:**1509-1513.

Kelly KJ, Williams WW, Jr., Colvin RB, Meehan SM, Springer TA, Gutierrez-Ramos JC, and Bonventre JV (1996) Intercellular adhesion molecule-1-deficient mice are protected against ischemic renal injury. *J Clin Invest* **97:**1056-1063.

Kobayashi Y, Fukami T, Higuchi R, Nakajima M, and Yokoi T (2012) Metabolic activation by human arylacetamide deacetylase, CYP2E1, and CYP1A2 causes phenacetin-induced methemoglobinemia. *Biochem Pharmacol* **84:**1196-1206.

Koga T, Fujiwara R, Nakajima M, and Yokoi T (2011) Toxicological evaluation of acyl glucuronides of nonsteroidal anti-inflammatory drugs using human embryonic kidney 293 cells stably expressing human UDP-glucuronosyltransferase and human

hepatocytes. *Drug Metab Dispos* **39:**54-60.

Kumada T, Tsuneyama K, Hatta H, Ishizawa S, and Takano Y (2004) Improved 1-h rapid immunostaining method using intermittent microwave irradiation: practicability based on 5 years application in Toyama Medical and Pharmaceutical University Hospital. *Mod Pathol* **17:**1141-1149.

Lagas JS, Sparidans RW, Wagenaar E, Beijnen JH, and Schinkel AH (2010) Hepatic clearance of reactive glucuronide metabolites of diclofenac in the mouse is dependent on multiple ATP-binding cassette efflux transporters. *Mol Pharmacol* **77:**687-694.

Lee MJ, Lee JK, Choi JW, Lee CS, Sim JH, Cho CH, Lee KH, Cho IH, Chung MH, Kim HR, and Ye SK (2012) Interleukin-6 induces S100A9 expression in colonic epithelial cells through STAT3 activation in experimental ulcerative colitis. *PLoS One* **7:**e38801.

Leonard EJ, Yoshimura T, Tanaka S, and Raffeld M (1991) Neutrophil recruitment by intradermally injected neutrophil attractant/activation protein-1. *J Invest Dermatol* **96:**690-694.

Ley K, Laudanna C, Cybulsky MI, and Nourshargh S (2007) Getting to the site of inflammation: the leukocyte adhesion cascade updated. *Nat Rev Immunol* **7:**678-689.

Mackenzie PI, Bock KW, Burchell B, Guillemette C, Ikushiro S, Iyanagi T, Miners JO, Owens IS, and Nebert DW (2005) Nomenclature update for the mammalian UDP glycosyltransferase (UGT) gene superfamily. *Pharmacogenet Genomics* **15:**677-685.

Miller FC, Schorr WJ, and Lacher JW (1983) Zomepirac-induced renal failure. *Arch Intern Med* **143:**1171-1173.

Mitjans M, Galbiati V, Lucchi L, Viviani B, Marinovich M, Galli CL, and Corsini E (2010) Use of IL-8 release and p38 MAPK activation in THP-1 cells to identify allergens and to assess their potency *in vitro*. *Toxicol In Vitro* **24:**1803-1809.

Miyashita T, Kimura K, Fukami T, Nakajima M, and Yokoi T (2014) Evaluation and mechanistic analysis of the cytotoxicity of the acyl glucuronide of nonsteroidal anti-inflammatory drugs. *Drug Metab Dispos* **42:**1-8.

Nakayama S, Atsumi R, Takakusa H, Kobayashi Y, Kurihara A, Nagai Y, Nakai D, and

Okazaki O (2009) A zone classification system for risk assessment of idiosyncratic drug toxicity using daily dose and covalent binding. *Drug Metab Dispos* **37:**1970-1977.

Nechemia-Arbely Y, Barkan D, Pizov G, Shriki A, Rose-John S, Galun E, and Axelrod JH (2008) IL-6/IL-6R axis plays a critical role in acute kidney injury. *J Am Soc Nephrol* **19:**1106-1115.

Nowell MA, Richards PJ, Fielding CA, Ognjanovic S, Topley N, Williams AS, Bryant-Greenwood G, and Jones SA (2006) Regulation of pre-B cell colony-enhancing factor by STAT-3-dependent interleukin-6 trans-signaling: implications in the pathogenesis of rheumatoid arthritis. *Arthritis Rheum* **54:**2084-2095.

O'Neill PJ, Yorgey KA, Renzi NL, Jr., Williams RL, and Benet LZ (1982) Disposition of zomepirac sodium in man. *J Clin Pharmacol* **22:**470-476.

Ramasamy R, Vannucci SJ, Yan SS, Herold K, Yan SF, and Schmidt AM (2005) Advanced glycation end products and RAGE: a common thread in aging, diabetes, neurodegeneration, and inflammation. *Glycobiology* **15:**16R-28R.

Ritter JK (2000) Roles of glucuronidation and UDP-glucuronosyltransferases in xenobiotic bioactivation reactions. *Chem Biol Interact* **129:**171-193.

Rowland A, Miners JO, and Mackenzie PI (2013) The UDP-glucuronosyltransferases: their role in drug metabolism and detoxification. *Int J Biochem Cell Biol* **45:**1121-1132.

Santos NA, Catao CS, Martins NM, Curti C, Bianchi ML, and Santos AC (2007) Cisplatin-induced nephrotoxicity is associated with oxidative stress, redox state unbalance, impairment of energetic metabolism and apoptosis in rat kidney mitochondria. *Arch Toxicol* **81:**495-504.

Sato M and Kondoh M (2002) Recent studies on metallothionein: protection against toxicity of heavy metals and oxygen free radicals. *Tohoku J Exp Med* **196:**9-22.

Sawamura R, Okudaira N, Watanabe K, Murai T, Kobayashi Y, Tachibana M, Ohnuki T, Masuda K, Honma H, Kurihara A, and Okazaki O (2010) Predictability of idiosyncratic drug toxicity risk for carboxylic acid-containing drugs based on the

chemical stability of acyl glucuronide. *Drug Metab Dispos* **38:**1857-1864.

Schiopu A and Cotoi OS (2013) S100A8 and S100A9: DAMPs at the crossroads between innate immunity, traditional risk factors, and cardiovascular disease. *Mediators Inflamm* **2013:**828354.

Shapiro L and Dinarello CA (1995) Osmotic regulation of cytokine synthesis i*n vitro*. *Proc Natl Acad Sci USA* **92:**12230-12234.

Shimizu S, Atsumi R, Itokawa K, Iwasaki M, Aoki T, Ono C, Izumi T, Sudo K, and Okazaki O (2009) Metabolism-dependent hepatotoxicity of amodiaquine in glutathione-depleted mice. *Arch Toxicol* **83:**701-707.

Silver EH and Murphy SD (1981) Potentiation of acrylate ester toxicity by prior treatment with the carboxylesterase inhibitor triorthotolyl phosphate (TOTP). *Toxicol Appl Pharmacol* **57:**208-219.

Skokowa J, Lan D, Thakur BK, Wang F, Gupta K, Cario G, Brechlin AM, Schambach A, Hinrichsen L, Meyer G, Gaestel M, Stanulla M, Tong Q, and Welte K (2009) NAMPT is essential for the G-CSF-induced myeloid differentiation via a NAD(+)-sirtuin-1-dependent pathway. *Nat Med* **15:**151-158.

Smith PC, McDonagh AF, and Benet LZ (1990) Effect of esterase inhibition on the disposition of zomepirac glucuronide and its covalent binding to plasma proteins in the guinea pig. *J Pharmacol Exp Ther* **252:**218-224.

Smith VT (1982) Anaphylactic shock, acute renal failure, and disseminated intravascular coagulation. Suspected complications of zomepirac. *JAMA* **247:**1172-1173.

Spahn-Langguth H and Benet LZ (1992) Acyl glucuronides revisited: is the glucuronidation process a toxification as well as a detoxification mechanism? *Drug Metab Rev* **24:**5-47.

Suzuki E, Yamamura N, Ogura Y, Nakai D, Kubota K, Kobayashi N, Miura S, and Okazaki O (2010) Identification of valproic acid glucuronide hydrolase as a key enzyme for the interaction of valproic acid with carbapenem antibiotics. *Drug Metab Dispos* **38:**1538-1544.

Takeuchi M, Takino J, Sakasai-Sakai A, Takata T, Ueda T, Tsutsumi M, Hyogo H, and

Yamagishi S (2014) Involvement of the TAGE-RAGE system in non-alcoholic steatohepatitis: Novel treatment strategies. *World J Hepatol* **6:**880-893.

Tanaka T and Kishimoto T (2014) The biology and medical implications of interleukin-6. *Cancer Immunol Res* **2:**288-294.

Tietze F (1969) Enzymic method for quantitative determination of nanogram amounts of total and oxidized glutathione: applications to mammalian blood and other tissues. *Anal Biochem* **27:**502-522.

Trauner M and Boyer JL (2003) Bile salt transporters: molecular characterization, function, and regulation. *Physiol Rev* **83:**633-671.

Usui T, Mise M, Hashizume T, Yabuki M, and Komuro S (2009) Evaluation of the potential for drug-induced liver injury based on in vitro covalent binding to human liver proteins. *Drug Metab Dispos* **37:**2383-2392.

Wang J, Davis M, Li F, Azam F, Scatina J, and Talaat R (2004) A novel approach for predicting acyl glucuronide reactivity via Schiff base formation: development of rapidly formed peptide adducts for LC/MS/MS measurements. *Chem Res Toxicol* **17:**1206-1216.

Wang M, Gorrell MD, McGaughan GW, and Dickinson RG (2001) Dipeptidyl peptidase IV is a target for covalent adduct formation with the acyl glucuronide metabolite of the anti-inflammatory drug zomepirac. *Life Sci* **68:**785-797.

Wells PG, Mackenzie PI, Chowdhury JR, Guillemette C, Gregory PA, Ishii Y, Hansen AJ, Kessler FK, Kim PM, Chowdhury NR, and Ritter JK (2004) Glucuronidation and the UDP-glucuronosyltransferases in health and disease. *Drug Metab Dispos* **32:**281-290.

Whelton A and Hamilton CW (1991) Nonsteroidal anti-inflammatory drugs: effects on kidney function. *J Clin Pharmacol* **31:**588-598.

Wieland E, Shipkova M, Schellhaas U, Schutz E, Niedmann PD, Armstrong VW, and Oellerich M (2000) Induction of cytokine release by the acyl glucuronide of mycophenolic acid: a link to side effects? *Clin Biochem* **33:**107-113.

Wung BS, Ni CW, and Wang DL (2005) ICAM-1 induction by TNFalpha and IL-6 is mediated

by distinct pathways via Rac in endothelial cells. *J Biomed Sci* **12:**91-101.

Yano A, Oda S, Fukami T, Nakajima M, and Yokoi T (2014) Development of a cell-based assay system considering drug metabolism and immune- and inflammatory-related factors for the risk assessment of drug-induced liver injury. *Toxicol Lett* **228:**13-24.

Zreiqat H, Belluoccio D, Smith MM, Wilson R, Rowley LA, Jones K, Ramaswamy Y, Vogl T, Roth J, Bateman JF, and Little CB (2010) S100A8 and S100A9 in experimental osteoarthritis. *Arthritis Res Ther* **12:**R16.

LIST OF PUBLICATIONS

This thesis is described based on the following publications

1. Iwamura A, Ito M, Mitsui H, Hasegawa J, Kosaka K, Kino I, Tsuda M, Nakajima M, Yokoi T, Kume T. (2015) Toxicological evaluation of acyl glucuronides utilizing half-lives, peptide adducts, and immunostimulation assays. *Toxicol In Vitro* **30**:241-249.

ACKNOWLEDGEMENTS

I would like to express my deepest appreciation and sincere gratitude to Professor Miki Nakajima and Professor Tsuyoshi Yokoi (Nagoya University Graduate School of Medicine) for their excellent supervision, guidance and constructive criticism throughout my research until the accomplishment of this PhD. I greatly appreciate Professors Ikumi Tamai, and Yukio Kato, and Associate Professors Takeo Nakanishi, and Tatsuki Fukami of Faculty of Pharmaceutical Sciences, Kanazawa University for valuable comments and suggestions as reviewers.

I am grateful to Masahito Ito, Hideaki Mitsui and Jun Hasegawa (Mitsubishi Tanabe Pharma Corporation) for technical assistance with dKF assay and DNA microarray analysis.

Finally, I wish to extend my thanks to Dr. Toshiyuki Kume, and all members of Division of Drug Metabolism and Toxicology, Kanazawa University and Division of Drug Safety Sciences, Nagoya University for sharing me a good time with many memorable experiences.